Metal ALD and Pulsed CVD: Fundamental Reactions and Links with Solution Chemistry

David J. H. Emslie, Preeti Chadha, Jeffrey S. Price

Department of Chemistry, McMaster University, 1280 Main Street West, Hamilton, ON, L8S 4M1, Canada.

Fax: (905) 522-2509. Tel: (905) 525-9140. E-mail: emslied@mcmaster.ca

----

Abbreviations: acac = acetylacetonate; AES = atomic emission spectroscopy; ALD = atomic layer deposition; allyl = C_3H_5; allyl^R = CH_2CRCH_2; allyl^{R2} = RCHCHCHR; amd^R = RNCMeNR amidinate; amd$^{R,R'}$ = RNCR'NR amidinate; ^{n}Bu = *n*-butyl; ^{s}Bu = *sec*-butyl; ^{t}Bu = *tert*-butyl; CHD = 1,3-cyclohexadiene; CMOS = complementary metal-oxide-semiconductor; COD = 1,5-cyclooctadiene; COT = cyclooctatetraene; Cp = cyclopentadienyl; Cp* = pentamethylcyclopentadienyl; Cp' = methylcyclopentadienyl; Cp^{Et} = ethylcyclopentadienyl; CVD = chemical vapour deposition; dmamb = 1-dimethylamino-2-methyl-2-butanolate ($OCMeEtCH_2NMe_2$); dppe = 1,2-bis(diphenylphosphino)ethane; DRAM = dynamic random-access memory; Et = ethyl; fod = 2,2-dimethyl-6,6,7,7,8,8,8-heptafluorooctane-3,5-dionate; hfac = 1,1,1,5,5,5-hexafluoroacetylacetonate; IPSA = *N*-isopropyl-2-salicylaldiminate; IR = infrared; LIALD = liquid injection ALD; LICVD = liquid injection CVD; Me = methyl; MIM = metal-insulator-metal; MOS = metal-oxide-semiconductor; nacnac^R = MeC(=NR)CHC(=NR)Me β-diketiminate; nacnac$^{cycle-R,R'}$ = R'C(=NR)CH{C=N(CH_2)$_3$}; NHC = *N*-heterocyclic carbene; od = 2,4-octanedionate; OTf = triflate; PEALD = plasma-enhanced ALD; Ph = phenyl; Pin = pinacolate ($OCMe_2CMe_2O$); ^{i}Pr = *iso*-propyl; PVD = physical vapour deposition; PyrIm^R = (NC_4H_3)CH=NR 2-pyrrolylaldimine; QCM = quartz crystal microbalance; QMS = quadrupole mass spectrometry; SAM = self-assembled monolayer; TEM = transmission electron microscopy; TFEL = thin film electroluminescent; thd = 2,2,6,6,-tetramethyl-3,5-heptanedionate; UHAR = ultra-high aspect ratio; UHV = ultra-high vacuum; VTMS = vinyltrimethylsilane; XPS = X-ray photoelectron spectroscopy.

Contents

Abstract

1 Introduction

1.1 Thermal ALD and pulsed-CVD

1.2 A brief introduction to metal ALD and pulsed-CVD

1.3 Precursor and co-reactant property requirements and their relationship to new ALD reaction chemistry development

1.4 Focus and scope of the review

2 Metal ALD and pulsed-CVD reactions organized by co-reactant

2.1 Dioxygen, air or ozone

2.2 Dihydrogen

2.3 Dioxygen, ozone or water, followed by dihydrogen

2.4 Main group hydrides (hydrosilanes, hydroboranes and hydroalanes)

2.5 Nitrogen-based co-reactants

2.5.1 Ammonia, with or without dihydrogen

2.5.2 Hydrazines

2.6 $C_xH_yO_z$ co-reactants

2.6.1 Formalin

2.6.2 Glyoxylic acid

2.6.3 Formic acid

2.6.4 Alcohols

2.7 Zinc metal

2.8 Diethylzinc

2.9 Trimethylaluminium

3 Solution reactivity studies applied to the rapid identification of promising new reaction chemistries for metal ALD

4 Concluding remarks

Acknowledgements

References

ABSTRACT

Atomic layer deposition (ALD) is a thin film deposition technique which operates *via* repeated alternating and self-terminating surface-based reactions between a precursor and a co-reactant, separated in time by purge steps. This technique is particularly well-suited to the deposition of highly uniform and conformal thin films, even on surfaces with nano-scale high aspect ratio features. Furthermore, use of a metal precursor *and* a co-reactant in ALD and the related technique of pulsed-CVD (pulsed-chemical vapour deposition), provides the potential for deposition of materials that may be inaccessible using CVD methods that rely upon the thermal decomposition of a single metal precursor. This review surveys the different classes of co-reactant used for thermal metal ALD/pulsed-CVD with a focus on the reaction chemistries known or proposed to be involved. Parallels are drawn between surface-based metal ALD/pulsed-CVD reactivity and solution-based reactivity including electroless deposition, solution-based nanoparticle synthesis, and the synthesis of zero-valent complexes bearing labile ligands. Also described are applications of solution screening and solution mechanistic studies to the identification of promising new ALD/pulsed-CVD reactivities, and the generation of initial mechanistic hypotheses as to the fundamental reaction steps involved in metal ALD/pulsed-CVD. A primary goal of this review is to provide a unique reactivity-based perspective of metal ALD/pulsed-CVD. In addition, we have endeavoured to illustrate commonalities between solution-based and surface-based reactions relevant to metal deposition, and to highlight beneficial applications of the former to the development of the latter.

Keywords: ALD; pulsed-CVD; metal deposition; reaction pathways; solution studies.

1. Introduction

1.1. Thermal ALD and pulsed-CVD

For many years, PVD and CVD have been central techniques for the deposition of thin metal films with a broad range of applications. However, the directional nature of these methods can lead to difficulties in: (a) obtaining ultra-thin films of uniform thickness, and (b) deposition of conformal films within nano-scale high aspect ratio features (e.g. trenches or vias), and these difficulties are becoming increasingly significant in the microelectronics industry as a result of rapidly decreasing device dimensions. Furthermore, while CVD offers improved conformality relative to PVD, it suffers from: (a) the potential for particle formation due to reactions occurring in the vapour phase rather than on the substrate surface, (b) in the case of solid precursors, dependence of film growth rate on precursor particle size, and (c) unavailability of precursors for deposition of certain materials, including many of the transition metals [1, 2].

ALD is a technique related to CVD which largely overcomes the limitations outlined above, although the overall deposition rate is generally much lower than that of CVD. In ALD, a volatile metal precursor is employed, as in CVD, but in this case, the substrate temperature and precursor thermal stability are such that the precursor does not undergo thermal decomposition upon contact with the substrate. Instead, deposition is achieved by repeated alternating self-terminating surface-based reactions between a metal precursor and a co-reactant [1-10]. In thermal ALD, the co-reactant is a ‘stable’ entity (e.g. H_2, H_2O, O_2 or O_3), while in plasma-enhanced ALD (PEALD), the co-reactant is plasma-generated (e.g. H, O or N atoms). Potential drawbacks of PEALD are that it introduces additional complexity to an ALD reactor, exposure to plasma-generated ions and UV-radiation can cause damage to the substrate and/or the growing film, and conformal deposition inside high aspect ratio features is difficult; this is especially the case for metal deposition using hydrogen plasma, since hydrogen radicals have particularly high recombination rates on most metal surfaces [11, 12]. On the other hand, a major advantage of PEALD is that it can be used to deposit a range of materials at low temperature, due to the high reactivity of species such as atomic hydrogen, oxygen and nitrogen. For example, while thermal ALD of silver metal has not yet been reported, PEALD of silver metal has been achieved using hydrogen plasma in combination with [(fod)Ag(PEt_3)] at 120 °C. The silver precursor was delivered at 105 °C, and undergoes surface-based thermal

decomposition above 140 °C [13], rendering it unsuitable as a candidate for thermal ALD of silver films using less reactive molecular hydrogen in place of atomic hydrogen. This example highlights a fairly general challenge in the development of new thermal metal ALD processes that rely on the existing suite of co-reagents; the availability of metal precursors with sufficiently high thermal stability and reactivity. PEALD is one way to utilize metal precursors of limited thermal stability, and the development of more reactive co-reagents for thermal ALD is another. In this review, only thermal ALD will be discussed, and from herein the term ALD is used to mean thermal ALD unless otherwise specified.

The reactions in ALD are designed to yield only volatile byproducts, and these, as well as excess metal precursor / co-reactant, are removed in inert gas purge steps between metal precursor and co-reactant pulses. The defining characteristic of ALD is that the metal precursor and the co-reactant are adsorbed and/or react with the surface in a *self-limiting* fashion. Therefore, so long as sufficient vapour doses of the metal precursor and co-reactant are delivered to ensure maximum surface coverage and complete reaction, the thickness of the deposited film will depend only on the number of precursor/purge/co-reactant/purge cycles, and the film will grow conformally on all exposed surfaces on which nucleation can occur, including the surfaces of high aspect-ratio features. If self-limiting behaviour cannot be achieved, even in cases where ALD reactivity is accompanied by a minor parasitic CVD process, the overall process is termed pulsed-CVD [1-10].

Although ALD offers advantages not conferred by pulsed-CVD, in both cases use of a metal precursor *and* a co-reactant provides access to a broader range of deposition chemistries than CVD involving thermal decomposition of a single metal precursor. Consequently, both ALD and pulsed-CVD provide the potential for deposition of materials that are inaccessible using single precursor CVD, as well as enhanced potential for the development of deposition reactions capable of operating at low temperature.

1.2. A brief introduction to metal ALD/pulsed-CVD

Relative to metal oxide and metal nitride ALD, examples of thermal metal ALD are far less common. In fact, as illustrated graphically in Figure 1 (see Section 2 of this review for references), thermal metal ALD has thus far only been achieved for the least electropositive

transition metals: the noble metals not including silver and gold, 1st row congeners of the noble metals, and the group 6 elements molybdenum and tungsten. Beyond this, pulsed-CVD has been reported for Ti/Al alloy (under UHV conditions), Mn, and Ag; *vide infra*.

3 Li 0.98	4 Be 1.57											5 B 2.04	6 C 2.55	7 N 3.04	8 O 3.44
11 Na 0.93	12 Mg 1.31											13 Al 1.61	14 Si 1.90	15 P 2.19	16 S 2.58
19 K 0.82	20 Ca 1.00	21 Sc 1.36	22 Ti 1.54	23 V 1.63	24 Cr 1.66	25 Mn 1.55	26 Fe 1.83	27 Co 1.88	28 Ni 1.91	29 Cu 1.90	30 Zn 1.65	31 Ga 1.81	32 Ge 2.01	33 As 2.18	34 Se 2.55
37 Rb 0.82	38 Sr 0.95	39 Y 1.22	40 Zr 1.33	41 Nb 1.6	42 Mo 2.16	43 Tc 1.9	44 Ru 2.2	45 Rh 2.28	46 Pd 2.20	47 Ag 1.93	48 Cd 1.69	49 In 1.78	50 Sn 1.96	51 Sb 2.05	52 Te 2.1
55 Cs 0.79	56 Ba 0.89	71 Lu 1.27	72 Hf 1.3	73 Ta 1.5	74 W 2.36	75 Re 1.9	76 Os 2.2	77 Ir 2.20	78 Pt 2.28	79 Au 2.54	80 Hg 2.00	81 Tl 2.04	82 Pb 2.33	83 Bi 2.02	84 Po 2.0
87 Fr 0.7	88 Ra 0.9	103 Lr --													

Ln	57 La 1.10	58 Ce 1.12	59 Pr 1.13	60 Nd 1.14	61 Pm --	62 Sm 1.17	63 Eu --	64 Gd 1.20	65 Tb --	66 Dy 1.22	67 Ho 1.23	68 Er 1.24	69 Tm 1.25	70 Yb --
An	89 Ac 1.1	90 Th 1.3	91 Pa 1.5	92 U 1.38	93 Np 1.36	94 Pu 1.28	95 Am 1.3	96 Cm 1.3	97 Bk 1.3	98 Cf 1.3	99 Es 1.3	100 Fm 1.3	101 Md 1.3	102 No 1.3

Figure 1. Periodic table, not including hydrogen, halogens and noble gases, highlighting metals that have been deposited by thermal ALD or pulsed-CVD (only reports in peer-reviewed literature are included; see section 2 for references). Metals that have been deposited by ALD are enclosed by solid black boxes. Metals (or alloys) that have been deposited only by pulsed-CVD are enclosed by dashed black boxes. Atomic numbers are shown above the atom symbols and Pauling electronegativities are shown below (for values with two decimal places, the oxidation state is: I for groups 1 and 11, II for groups 2, 4-10 and 12, III for groups 3 and 13, and IV for group 14) [14]. Non-metals (including semi-metals) and elements without significant natural abundance are shown in white. The remaining elements are shaded.

From the above discussion, it follows that a major challenge in ALD is the development of suitable reaction chemistry for deposition of metals not yet accessed by ALD. However, even for metals that have previously been accessed by ALD, various features of the precursors, the

deposition process and/or the resulting films may prevent commercial application. These include: (a) difficulties in precursor scale-up, (b) insufficient precursor or co-reactant thermal stability, (c) an ALD temperature that is too high to be compatible with the desired substrate (temperatures of 200-400 °C are common; *vide infra*), (d) an ALD temperature that causes agglomeration of thin metal films [15, 16], (e) deposition of metal films containing impurities at levels that are unacceptable for the target application, (f) impractical or complex and costly deposition conditions (e.g. those involving extremely long pulse or purge durations, an unacceptably low growth rate, a very narrow ALD temperature window, injection of the precursor or co-reactant as a solution, or UHV deposition conditions), (g) an unacceptably long induction period prior to the onset of self-limiting film growth [3, 17], (h) film growth that does not lead to continuous films at low film thicknesses (island growth) [3, 7], (i) film morphologies that do not provide the desired physical properties and performance, (j) poor adhesion between the deposited film and the underlying substrate, and (k) deposition of films that do not have the desired crystalline phase, crystal orientation, or level of crystallinity. Which of these potential limitations are relevant will depend on the metal being deposited and the target application.

Limitations (b)-(e) above can be related fairly directly to precursor, co-reactant and reaction byproduct volatility/thermal stability, and the reaction pathways occurring at the surface. By contrast, limitations (g-k) will be substrate specific and are less directly linked to the fundamental classes of chemical reaction involved in metal deposition. The development of new ALD methods that overcome limitations such as those outlined above is clearly an important goal, although in the case of substrate-specific behaviour the development of multiple fundamentally different reaction chemistries, each with a different substrate scope may be required. New ALD reaction chemistries that allow for straightforward and controlled addition of specific impurities *via* an ALD mechanism may also be of interest. Furthermore, substrate-selective ALD/pulsed-CVD of metals (e.g. deposition on Pd and/or Pt rather than an glass, silica or a metal oxide surface [18, 19], on H-terminated Si rather than OH-terminated SiO_2 [20], or on substrates patterned with self-assembled polymer monolayers) [21-29] is an active field of research with its own deposition chemistry requirements.

Metals deposited by ALD have a broad range of potential applications in the fields of microelectronics (microprocessors, memory devices etc.), flat panel displays, fuel-cells, solar

cells, and catalysis [1, 7]. In the area of microelectronics, various potential applications of ALD metal films have been cited in the literature. These include [7]: rear electrode materials for inverted TFEL devices or plugs for the UHAR contacts of advanced DRAM (Mo, W) [30, 31], positive channel MOS gate electrodes (Re, Ru, Rh, Ir, Pd, Pt) [23], electrode materials in MIM capacitors for future DRAM (Ru, Ir) [2, 32-34], nanocrystals for non-volatile nanocrystal memory (W, Ru, Pd, Au) [7], diffusion barriers, adhesion layers or seed layers for copper deposition (Ru, Os, Rh and others) [32-36], precursors to $CoSi_2$, NiSi or PtSi source and drain materials to replace $TiSi_2$ in MOS devices (generated by annealing Co, Ni or Pt metal films on silicon substrates) [20, 37-41], gate materials for CMOS devices (Pt) [40], and interconnect wiring (Cu or Ag) [13, 42].

1.3. Precursor and co-reactant property requirements and their relationship to new ALD reaction chemistry development

ALD, and to a lesser extent pulsed-CVD, place strict requirements on the physical and chemical properties of metal precursors and co-reactants. In particular, metal precursors and co-reactants should exhibit:

- Volatility such that the delivery temperature of the compound is below the substrate temperature, to avoid problems with precursor condensation (for solid precursors used with an ALD reactor operating under non-UHV conditions, typical vapor pressures at the delivery temperature are in the 0.01 to 10 Torr range, preferably at least 0.1 Torr [1]). It is also preferable that the precursor and co-reactant are sufficiently volatile to allow low-temperature ALD/pulsed-CVD if the reactivity between the precursor, the co-reactant, and the substrate is such that this can be achieved.
- For ALD, sufficiently high metal precursor and co-reactant thermal stability and reactivity to ensure that ALD can be achieved at temperatures below the onset of CVD (the larger the ALD window, the better). A similar criterion will in some cases apply to pulsed-CVD.

- Long-term thermal stability at the delivery temperature.
- ALD/pulsed-CVD reactivity that yields only volatile byproducts.
- Surface reactivity which allows adsorption and film growth on both the substrate (in initial stages of film deposition) and the growing film.
- Scaleable syntheses with reasonable overall yields.
- Low melting points are also desirable, since the use of liquid precursors and co-reactants helps to avoid particle incorporation and to ensure uniformity in the amount of precursor and co-reactant delivered in each pulse (for solids, the amount of precursor or co-reactant delivered in each pulse depends on particle size, which can vary significantly as precursor / co-reactant is consumed). With respect to the latter point, use of liquid precursors and co-reactants is less critical for ALD than for thermal CVD, since film thickness will depend only on the number of reaction cycles, providing that sufficiently long precursor and co-reactant pulses are employed.

These requirements unavoidably curtail the complexity of ALD precursors and co-reactants. However, by the same token, the development of new ALD reactivity that is compatible with precursors and co-reactants that meet the above criteria presents a substantial challenge. This is especially the case for more difficult targets (e.g. metals currently inaccessible by ALD or low temperature ALD reactivities), and in many cases the development of new ALD reactivity must go hand in hand with the design of new precursors able to meet the requirements of the target reactivity.

1.4. Focus and Scope of the Review

This review aims to highlight the different classes of co-reactant used for metal ALD/pulsed-CVD, and to discuss the reaction pathways known or proposed to be involved. Where appropriate, parallels are drawn between ALD/pulsed-CVD reactivity and solution-based reactivity, including electroless metal deposition, solution-based metal nanoparticle synthesis,

and the synthesis of zero-valent complexes bearing labile ligands. Also discussed are applications of solution studies towards the development and study of potential new ALD/pulsed-CVD reaction chemistries, and our research in the field of copper metal deposition is used to highlight these applications. It is hoped that this review will provide a unique reactivity-based perspective of metal ALD, and will highlight the value of solution studies; both for the development of new ALD reaction chemistries and as a comparatively straightforward means to generate initial mechanistic hypotheses as to the fundamental reaction steps involved in metal ALD. As stated in section 1.1, only thermal methods for ALD and pulsed-CVD are included in this review. Additionally, the review focuses only on deposition reactions reported in the peer-reviewed literature.

2. Metal ALD and Pulsed-CVD Reactions Organized by Co-reactant

Reaction chemistries utilized for metal ALD/pulsed-CVD are described below, organized according to the type of co-reactant: [a] O_2 (including air) and O_3, [b] H_2, [c] O_2, O_3 or H_2O followed by H_2 [d] main group hydrides (hydrosilanes, hydroboranes and hydroalanes), [e] amines and hydrazines, [f] $C_xH_yO_z$ organic molecules (formaldehyde, glyoxylic acid, formic acid, and alcohols), [g] Zn metal, [h] $ZnEt_2$ and [i] $AlMe_3$. In each section, the first paper(s) detailing the use of a novel precursor / co-reactant combination for metal ALD are tabulated. Pulsed-CVD reactions (or CVD reactions for which the use of a reactive carrier gas such as H_2 allows deposition to occur at a significantly lower temperature) are included only in select cases where the reaction chemistry or the deposited metal differs significantly from that currently accessible by ALD. In each section, one or two representative examples are discussed in more detail in order to highlight the primary reactions found or hypothesized to be involved in metal deposition.

2.1. Dioxygen, air or ozone

The noble metals are strongly resistant to bulk oxidation. However, molecular O_2 can reversibly adsorb and dissociate on their surfaces (the latter process is significantly less

favorable on gold) [43-45], providing access to reactive oxo species. As a consequence, O_2 (pure, diluted in argon, or air), and in some cases O_3 may be used to effect pure metal deposition (Table 1). This strategy has been employed most often for iridium, platinum and ruthenium ALD, and several illustrative examples are discussed below. Addition of a strong oxidizing agent (O_2 or O_3) to effect metal reduction is at first glance counter-intuitive, but *overall* it is the ligands that are oxidized, and this typically occurs at least to some extent by combustion to release CO_2 and/or CO and H_2O.

For the precursor [Ir(acac)$_3$], iridium metal ALD has been reported in the 225-375 °C range using air or O_2 as the co-reactant [46, 47]. Iridium ALD was also achieved using more reactive O_3 at 210-225 °C, although at lower temperatures (165-200 °C) only IrO_2 was deposited [48]. The mechanism for Ir ALD using [Ir(acac)$_3$] and O_2 at 300 °C has been studied using QCM and QMS, leading to the following proposed reaction steps: (1) Reaction of [Ir(acac)$_3$] with adsorbed oxygen species on the growing ALD iridium surface, releasing 1-2 of the acac ligands as acetylacetone (proposed to involve reaction with surface hydroxyl groups, although alternative reactivities can be considered; *vide infra*) and approximately 0.1 ligand through combustion. (2) Release of remaining acetylacetonate ligands by combustion during the subsequent O_2 exposure, and repopulation of the iridium surface with oxygen species [47]. Presumably Ir ALD using [Ir(acac)$_3$] and O_3 operates by an analogous mechanism, and the switch from iridium metal ALD at 210 °C to IrO_2 ALD at 200 °C suggests that step 1 above ceases to operate effectively at low temperatures [48].

QCM and QMS studies of Pt ALD using [Cp'PtMe$_3$] and O_2 led to similar conclusions with 1.6 of the 3 methyl groups eliminated as CH_4 during the metal precursor pulse [47]. However, it has recently been proposed that the source of hydrogen for methane elimination in this step of the reaction is ligand dehydrogenation on the catalytically active platinum surface, rather than surface hydroxyl groups [49]. QMS studies also recently revealed that in Ru ALD using [CpRuEt(CO)$_2$] at 325 °C, surface chemisorption of the metal precursor resulted in the formation of combustion products (CO_2, CO and H_2O) *and* a substantial quantity of H_2. By contrast, during the O_2 pulse, no H_2O or other H-containing byproducts were detected. These observations can be rationalized by the following two steps: (1) The metal precursor adsorbs on the substrate surface (Ru with adsorbed oxygen atoms), a fraction of the ligands react with surface oxygen to form combustion products, and the remainder undergo dehydrogenation with

release of H_2 into the gas phase. This results in a buildup of carbon (~30% of the carbon atoms in [$CpRuEt(CO)_2$]) on the substrate surface. (2) The subsequent O_2 pulse removes carbon from the ruthenium surface, releasing it as CO_2 and CO, and oxygen-coverage of the ruthenium surface is re-established. The authors noted that the heterogeneous catalysis and surface science literature contains many reports of dehydrogenation reactivity on noble metals such as Ir, Pt and Ru, so it follows that this reactivity may operate in other noble metal ALD processes involving organic ligands [50].

Table 1. Metal precursor / co-reactant combinations that have been used for metal ALD or pulsed-CVD and employ O_2 or O_3 as the co-reactant (not in combination with H_2). This table focuses on initial literature reports for each metal precursor / co-reactant combination. The first column of the table indicates whether ALD or pulsed-CVD is claimed, although in many cases ALD is claimed without demonstration of self-limiting growth.

Deposited Metal (ALD or CVD)	Substrate	Metal Precursor	Co-reactant	Reaction Temp. (°C)	Year	Reference
Ru (ALD)	Al_2O_3, TiO_2, glass	$RuCp_2$	O_2	275-400	2003	Aaltonen *et al.* [51]
Ru (LIALD)	C nanotubes	$Ru(od)_2$	O_2	325-375	2003	Min *et al.* [52]
Ru (CVD)	HfO_2	$(thd)_2Ru(COD)$	O_2	280-320	2003	Dey *et al.* [53, 54]
Ru (ALD)	Al_2O_3	$Ru(thd)_3$	O_2	325-450	2004	Aaltonen *et al.* [55]
Ru (ALD)	TiN	$Ru(Cp^{Et})_2$	O_2	270	2004	Kang *et al.* [56]
Ru (LIALD)	Si, SiO_2, TiO_2, TiN	$(Cp^{Et})Ru$(2,4-dimethylpentadienyl)	O_2	230-280	2007	Hwang *et al.* [57]
Ru (ALD)	SiO_2, TiN	$(C_6H_4Me^iPr\text{-}p)Ru(CHD)$	O_2	220	2009	Kim *et al.* [58]
Ru (ALD)	Si, SiO_2, Al_2O_3, TiO_2, ZrO_2, HfO_2	$Cp'RuCp^{Et}$	O_2	250-325	2010	Kukli *et al.* [59]
Ru (ALD)	Al_2O_3	$CpRu\{C_5H_4(CHMeNMe_2)\}$	air	325-500	2010	Ritala *et al.* [60]
Ru (ALD)	H-term Si	$CpRuEt(CO)_2$	O_2	300	2010	Chabal *et al.* [61]
Ru (ALD)	H-term Si, SiO_2, ZrO_2, TiN	$(Cp^{Et})Ru$(pyrrolyl)	air or O_2	275-350	2011	Ritala *et al.* [62]
Ru (ALD)	H-term Si, SiO_2, Al_2O_3, HfO_2, TiO_2	$Ru(NC_4H_2Me_2\text{-}2,5)_2$	O_2	250-300	2012	Kukli *et al.* [63]
Os (ALD)	Al_2O_3	$OsCp_2$	O_2	325-375	2011	Hämäläinen *et al.* [35]
Rh (ALD)	Al_2O_3	$Rh(acac)_3$	O_2	200-250	2005	Ritala *et al.* [36]
Ir (ALD)	Al_2O_3 or TiN	$Ir(acac)_3$	air or O_2	225-375 (air), 300 (O_2)	2004, 2010	Ritala *et al.* [46] Elam *et al.* [47]
Ir (CVD)	Si	$Ir(CO)_2\{OC(CF_3)_2CH_2CMe{=}N^iPr\}$	O_2 (0.5 Torr)[a]	325-400	2006	Chi and Carty *et al.* [64]
Ir (ALD)	SiO_2 (on Si)	$(Cp^{Et})Ir(COD)$	O_2 (<70% in Ar, 1 Torr)[a]	230-290	2008	Kang *et al.* [65]
Ir (ALD)	SiO_2 or Al_2O_3	$Ir(acac)_3$	O_3	210-225	2008	Hämäläinen *et al.* [48]
Ir (ALD)	Al_2O_3	$Cp'Ir(CHD)$	O_2	225-300	2010	Hämäläinen *et al.* [66]
Pd (LICVD)	Al_2O_3 or Ir	$Pd\{OC(CF_3)CHC(CF_3)N^nBu\}_2$	O_2	250-275	2004	Aaltonen *et al.* [67]
Pt (ALD)	Al_2O_3 or Ir	$Cp'PtMe_3$	air or O_2	300 for air, 200 for pure O_2	2003-2004	Aaltonen *et al.* [67, 68]
Pt (ALD)	Al_2O_3	$Pt(acac)_2$	O_3	140	2008	Hämäläinen *et al.* [69]

(a) At higher concentrations of O_2 and/or higher deposition pressures, IrO_2 was deposited, rather than Ir metal.

2.2. Dihydrogen

Given the reducing nature of H_2, it is an obvious choice as a co-reactant for metal ALD (Table 2), although its practical utility is limited by undesirable reactivity between H_2 and various substrates, especially many metal oxides [2, 70, 71]. Palladium metal ALD has been achieved using H_2 at particularly low temperatures as a result of the facile dissociation of H_2 to hydrogen atoms on the growing palladium surface [72, 73]. By contrast, most other metals only undergo ALD with H_2 at high temperatures (250-400 °C); some exceptions have been reported for ruthenium and copper. Pulsed-CVD of metallic manganese is particularly notable since manganese is significantly more electropositive than the other transition metals in Table 2 [74]. A well-characterized example of metal ALD using H_2 as the co-reactant is discussed below.

The reactions involved in copper metal deposition using $[Cu_2(amd^{sBu})_2]$ and H_2 have been studied on OH-terminated SiO_2 using XPS and IR spectroscopy [42]. At 185 °C, initial surface reactivity takes place between the copper precursor and surface OH groups to form Si-O-Cu bonds, releasing one equivalent of $H(amd^{sBu})$ per $[Cu_2(amd^{sBu})_2]$ precursor. The subsequent H_2 pulse releases most of the remaining amidinate ligands as $H(amd^{sBu})$, yielding copper atoms which can migrate and agglomerate to form copper particles. Cu-H bonds are expected to be formed *en route* to copper metal but were not detected, likely due to a low IR cross section or a short lifetime (H atoms have a high recombination probability on copper) [11]. Reaction of a portion of the liberated $H(amd^{sBu})$ with remaining OH groups on the silica surface [Si-OH + ^{s}BuNH-CMe=N^{s}Bu → Si-O-CMe(NH^{s}Bu)$_2$] may or may not occur. An IR mode at 1605 cm^{-1} which grows in intensity during H_2 exposures and loses intensity upon $[Cu_2(amd^{sBu})_2]$ addition was attributed to surface [Cu]-N^{s}Bu-CHMe-NH^{s}Bu linkages formed as a result of amidinate anion hydrogenation [42, 75]. However, it is notable that at the lower temperature of 120 °C, the reaction of neat liquid $[Cu_2(amd^{sBu})_2]$ with hydrogen yielded only copper metal and $H(amd^{sBu})$ [76].

Table 2. Metal precursor / co-reactant combinations that have been used for metal ALD or pulsed-CVD and employ H_2 as the co-reactant (not in combination with O_2, O_3 or H_2O). This

table focuses on initial literature reports for each metal precursor / co-reactant combination. The first column of the table indicates whether ALD or pulsed-CVD is claimed, although in many cases ALD is claimed without demonstration of self-limiting growth.

Deposited Metal (ALD or CVD)	**Substrate**	**Metal Precursor**	**Co-reactant**	**Reaction Temp. (°C)**	**Year**	**Reference**
Mn (CVD)	various	$Mn(amd^{iPr,nBu})_2$	H_2	300	2010	Gordon *et al.* [77]
Fe (ALD)	Si, C, glass, WN	$Fe_2(amd^{tBu})_2$	H_2	250	2003	Gordon *et al.* [78, 79]
Ru (CVD)	SiO_2 or Al_2O_3	$Ru(thd)_3$	H_2	140	2003	Lashdaf *et al.* [80]
Ru (ALD)	SiO_2	$Ru(acac)_3$	H_2	300-370	2007	Gelfond *et al.* [81]
Co (ALD)	Si, C, glass, WN	$Co_2(amd^{iPr})_2$	H_2	350	2003	Gordon *et al.* [78, 79]
Rh (CVD)	SiO_2	$\{RhCl(CO)_2\}_2$	H_2	100	1995	Kalck *et al.* [82, 83]
Rh (CVD)	SiO_2	$Rh(allyl)_3$	H_2	80	1995	Kalck *et al.* [82, 83]
Rh (CVD)	SiO_2	$(acac)Rh(CO)_2$	H_2	100	1995	Kalck *et al.* [82, 83]
Ir (ALD)	SiO_2	IrF_6	H_2	375	2005	Dussarrat *et al.* [84]
Ni (ALD)	Ti or Al	$Ni(acac)_2$	H_2	250	2000	Niinistö *et al.* [85]
Ni (ALD)	Si, C, glass, WN	$Ni_2(amd^{iPr})_2$	H_2	250	2003	Gordon *et al.* [78, 79]
Pd (ALD)	Ir or Pd	$Pd(hfac)_2$	H_2	80	2003	Senkevich *et al.* [86]
Pd (CVD)	SiO_2 or Al_2O_3	$Pd(thd)_2$	H_2	90	2003	Lashdaf *et al.* [80]
Pd (ALD)	Air oxidized Ta	$Pd(hfac)_2$	H_2	80	2006	Lu *et al.* [87]
Pd (CVD)	glass or silica powder	(hfac)Pd(allyl)	H_2	45-60	1996	Kalck *et al.* [83, 88, 89]
Pd (CVD)	glass or silica powder	CpPd(allyl)	H_2	30-60	1996	Kalck *et al.* [83, 88, 89]
Pt (CVD)	glass or silica powder	$PtMe_2(COD)$	H_2	90	2000	Kalck *et al.* [83, 89]
Pt (CVD)	Ti, Al, SiO_2	$Pt(acac)_2$	H_2	250	2000	Niinistö *et al.* [85]
Cu (ALD)	Ta	CuCl	H_2	360-410	1997	Mårtensson *et al.* [90]
Cu (ALD)	Pd/Pt, TiN, ITO, Ta, Fe or Ni	$Cu(thd)_2$	H_2	190-260	1998	Mårtensson *et al.* [18]
Cu (nd)[a]	Ti or Al	$Cu(acac)_2$	H_2	250	2000	Niinistö *et al.* [85]
Cu (ALD)	Si, C, glass, or Co on WN	$Cu_2(amd^{iPr})_2$	H_2	280	2003	Gordon *et al.* [78, 79]
Cu (ALD)	SiO_2, Si_3N_4, Co, WN	$Cu_2(amd^{sBu})_2$	H_2	190	2005	Gordon *et al.* [76, 91]
Cu (nd)[a]	TiN	$Cu(hfac)_2$	H_2, pyridine	25-100	2010	Chang *et al.* [92]

(a) nd = not determined.

2.3. Dioxygen, ozone or water, followed by dihydrogen

As described in section 2.1, reaction of [$Ir(acac)_3$] with O_3 at temperatures at or below 200 °C resulted in IrO_2 deposition, rather than iridium metal deposition [48]. However, iridium metal ALD could be achieved below 200 °C if each O_3 pulse was followed by an H_2 pulse to reduce IrO_2 [93], and Ir ALD was achieved at 120-180 °C using [Cp'Ir(CHD)] followed by sequential O_3 and H_2 pulses (Table 3) [94]. Along similar lines, copper ALD was achieved using cycles of a CuCl pulse followed by an H_2O pulse and then an H_2 pulse (Table 3). The H_2O pulse is suggested to form Cu_2O and the H_2 pulse then converts Cu_2O to Cu [95]. A related nickel

metal deposition process was reported using sequential pulses of [$NiCp_2$], H_2O and hydrogen plasma at 165 °C. The first two pulses were shown to deposit a NiO film which was converted to nickel metal upon exposure to hydrogen plasma [96]. In several instances, metal films have been deposited in two separate non-alternating steps using related reaction chemistry (Table 3). For example [97], NiO ALD was achieved using [$Ni(acac)_2$] and O_3 at 250 °C, and the resulting film was reduced to nickel metal with H_2 at 230-500 °C. However, reduction of the NiO film to nickel metal caused structural collapse of the film and pinhole formation [85].

Table 3. Metal precursor / co-reactant combinations that have been used for metal ALD or pulsed-CVD and employ both (a) O_2, O_3 or H_2O, and (b) H_2 as co-reactants. This table focuses on initial literature reports for each metal precursor / co-reactant combination. The first column of the table indicates whether ALD or pulsed-CVD is claimed, although in many cases ALD is claimed without demonstration of self-limiting growth.

Deposited Metal (ALD or CVD)	Substrate	Metal Precursor	Co-reactant	Reaction Temp. (°C)	Year	Reference
Ir (ALD)	SiO_2, Al_2O_3 or glass	$Ir(acac)_3$	O_3, then H_2	165-200	2009	Hämäläinen *et al.* [93]
Ir (ALD)	Al_2O_3	Cp'Ir(CHD)	O_3, then H_2	120-180	2011	Hämäläinen *et al.* [94]
Cu (ALD)	Al_2O_3, SiO_2	CuCl	H_2O, then H_2	375-475	2004	Törndahl *et al.* [95]
Ni (ALD but step 2 involves plasma)	TiN	$NiCp_2$	H_2O, then H-plasma	165		Kang *et al.* [96]
Ni (stepwise)[a]	glass	$Ni(acac)_2$	O_3, then H_2	(1) 250, (2) 230-500	2000	Niinistö *et al.* [85]

(a) Stepwise metal film deposition by deposition of a metal oxide film, followed by chemical reduction of the film. Separate co-reactants and temperatures are given for each of these steps.

2.4. Main group hydrides (hydrosilanes, hydroboranes and hydroalanes)

In solution-phase organometallic chemistry, hydrosilanes such as Et_2SiH_2 and $PhSiH_3$ are often employed as reagents for the conversion of metal alkyl complexes to metal hydrides[98] (although in some cases metal silyl complexes are formed) [99], and in rare cases metal amido complexes have participated in analogous reactivity with hydrosilanes [100, 101]. These reactions are typically considered to follow σ-bond metathesis or oxidative addition/reductive elimination pathways, and similar elementary reaction steps can be envisaged for the

generation of unstable metal hydrides in metal ALD. Indeed H_2SiEt_2 has been employed as a co-reactant for Cu ALD, Si_2H_6 has been used for Mo and W deposition, and SiH_4 has been used for W ALD. Furthermore, the group 13 element hydrides B_2H_6 and $AlH_3(NMe_3)$ have been employed as co-reactants for metal deposition; the former for W ALD and the latter for Ti/Al pulsed-CVD under UHV conditions (Table 4). The overall reactions considered to be involved in Ti/Al pulsed-CVD are: (1) 3 $TiCl_4$ + 4 $AlH_3(NMe_3) \rightarrow$ 3 Ti + 6 H_2 + 4 $AlCl_3$ + 4 NMe_3, and (2) $AlH_3(NMe_3) \rightarrow$ Al + 1.5 H_2 + NMe_3 [102].

Tungsten ALD from WF_6 and Si_2H_6 has been studied by QCM, IR spectroscopy, mass spectrometry, AES and XPS, and at a temperature of 200 °C the proposed surface reactions are shown in equations 1-3 ([W] denotes the tungsten surface). This sequence of reactions leads to the formation of SiF_4 during the WF_6 pulse and $SiHF_3$ during the Si_2H_6 pulse, which matches experimental observations. However, the mechanism by which each of these steps occurs is not known. The reaction with WF_6 is self-limiting, while the reaction with Si_2H_6 is not, perhaps due to Si_2H_6 insertion into surface Si-H bonds; this CVD component is not accounted for in equations 1-3 [103, 104].

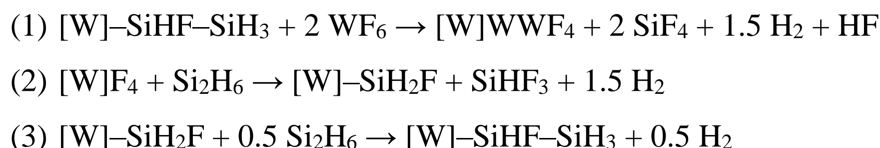

(1) $[W]\text{–}SiHF\text{–}SiH_3 + 2\ WF_6 \rightarrow [W]WWF_4 + 2\ SiF_4 + 1.5\ H_2 + HF$

(2) $[W]F_4 + Si_2H_6 \rightarrow [W]\text{–}SiH_2F + SiHF_3 + 1.5\ H_2$

(3) $[W]\text{–}SiH_2F + 0.5\ Si_2H_6 \rightarrow [W]\text{–}SiHF\text{–}SiH_3 + 0.5\ H_2$

ALD of Mo films was also achieved at 120 °C using MoF_6 in combination with Si_2H_6. Interestingly, films grown in a high vacuum reactor did not contain silicon impurities, while those grown in a viscous flow reactor contained around 20 at% Si impurities. Furthermore, in the Mo deposition reaction, exposure to Si_2H_6 led to mass loss, while in the analogous W ALD reaction, exposure to Si_2H_6 led to mass gain. These differences are indicative of different reaction mechanisms for Mo and W film growth [105]. In contrast to metal deposition reactions employing group 6 hexafluoride precursors, attempted deposition of metallic Ta by reaction of TaF_5 with Si_2H_6 yielded $TaSi_x$ ($x \sim 2$) [106, 107].

A recent method for low temperature copper metal deposition involved the use of two co-reactants; each reaction cycle involved pulsing with pyrazole, followed by the copper(II) precursor, and then H_2SiMe_2 [108]. This approach allowed copper metal deposition on both Au

and Ru substrates at the very low temperature of 45 °C. The initial reaction must involve coordination of pyrazole (without deprotonation) to the metal surface, and the following pulse of [(nacnac^H)Cu(VTMS)] is considered to release H(nacnac^H), thereby forming a copper(I) species bound to the substrate surface *via* a pyrazolyl anion (the presence of a surface-bound copper(I) species was confirmed by XPS, and it is this species that is reduced in the H_2SiMe_2 pulse). The authors drew a parallel between the role of pyrazole in this process and the role of hydroxyl groups in the deposition of Al_2O_3 films. However, they noted that unlike surface hydroxyl groups, the pyrazole molecule is not incorporated into the film. According to the patent literature, this general process can be extended to other metals (Co and Ru; possibly also Ni, Pd, Pt, Ir, W and Ta) [109-112].

Table 4. Metal precursor / co-reactant combinations that have been used for metal ALD or pulsed-CVD and employ main group hydride co-reactants. This table focuses on initial literature reports for each metal precursor / co-reactant combination. The first column of the table indicates whether ALD or pulsed-CVD is claimed, although in many cases ALD is claimed without demonstration of self-limiting growth.

Deposited Metal (ALD or CVD)	Substrate	Metal Precursor	Co-reactant	Reaction Temp. (°C)	Year	Reference
Cu (decomp)[a]	glass	Cu(PyrIm^{Ph})$_2$	H_2SiEt_2	160-170	2004	Grushin *et al.* [113]
Cu (decomp)[a]	SiO_2	Cu(nacnac$^{cycle\text{-}Me,Me}$)$_2$	H_2SiEt_2	100	2005	Park *et al.* [114]
Cu (decomp)[a]	Au	(nacnac$^{cycle\text{-}H,Me}$)Cu(VTMS)	H_2SiEt_2	120	2006	Park and Thompson *et al.* [115]
Cu (ALD-like)[c]	Au or Ru	(nacnac^H)Cu(VTMS)	pyrazole then H_2SiMe_2	45	2012	Thompson *et al.* [108]
Mo (ALD)[b]	Si or Al_2O_3	MoF_6	Si_2H_6	120-180	2011	George *et al.* [105]
W (ALD)	Pretreated SiO_2 or Mo	WF_6	Si_2H_6	150-325	2000	George *et al.* [103, 116]
W (CVD)	Pretreated SiO_2 or TiN	WF_6	SiH_4	300	2002-05	Kim *et al.* and others [117]
W with some B (ALD)	Pretreated SiO_2 or TiN	WF_6	B_2H_6	300	2002-05	Kim *et al.* and others [117]
Ti-Al (UHV-CVD)	Cu	$TiCl_4$	$AlH_3(NH_3)$	65-127 °C	1998	Kodas *et al.* [102]

(a) limited details were provided; most likely the solid precursor was exposed to H_2SiEt_2 vapours. (b) films grown in a high vacuum reactor did not contain silicon impurities, while those grown in a viscous flow reactor contained ~20 at% Si impurities. (c) ALD-like conformal deposition was achieved, but pyrazole did not show self-limiting adsorption, the copper precursor did not appear to react with all of the available surface-bound pyrazole (even using 15-20 second precursor pulses), and the deposition rate was higher than that expected for an ALD process.

2.5. Nitrogen-based co-reactants

2.5.1. Ammonia, with or without dihydrogen

Compared with H_2 and main group hydrides ($R_xE^{\delta+}–H^{\delta-}$), amines ($R_2N^{\delta-}–H^{\delta+}$) are perhaps less obvious choices as reducing co-reactants. However, NH_3 has been used for nickel metal ALD from [Ni(dmamb)$_2$] at 300 °C [29], ruthenium metal ALD from [(amd$^{t\mathrm{Bu}}$)$_2$Ru(CO)$_2$] at 300 °C (accompanied by ruthenium CVD) [118], and cobalt metal ALD from [Co(amd$^{i\mathrm{Pr}}$)$_2$] at 350 °C (Table 5) [28]. Futhermore, copper metal deposition was likely achieved from [Cu$_2$(amd$^{s\mathrm{Bu}}$)$_2$] at 280 °C using NH_3 [119], and from [Cu(hfac)$_2$] at 283 °C using pulses of H_2O followed by NH_3 (the H_2O pulse was required to initiate deposition on the oxide substrates; the resulting film was a mixture of Cu and Cu_3N; Table 5) [120]. Taking into consideration the polarity of N–H bonds, and the fact that NH_3 is the standard co-reactant for metal nitride ALD, it seems safe to assume that these reactions yield metal nitrides which decompose thermally under the reaction conditions; CoN has been reported to decompose to Co at approximately 300 °C (*via* Co_2N and Co_3N) [121], Ni_3N decomposes to Ni at 300 °C [122], Cu_3N decomposes readily to Cu above 200 °C (or more slowly under vacuum at 100 °C) [123], and RuN decomposes to Ru metal above around 100 °C [124, 125].

Ammonia, in combination with H_2, has also been used to prepare metallic Cu films at temperatures below 250 °C: (a) Cu_3N ALD was achieved using [Cu$_2$(amd$^{s\mathrm{Bu}}$)$_2$] and NH_3 at 160 °C, and treatment of the resulting film with H_2 at 225 °C provided copper metal [119], and (b) the reaction of [Cu(PyrIm$^{\mathrm{R}}$)$_2$] (R = Me or Et) with a 1:1 mixture of H_2 and NH_3 at 180 °C was reported to be more effective for copper metal deposition than the analogous reactions with H_2 or NH_3 alone (Table 5) [113].

The mechanisms of metal ALD reactions involving NH_3 do not appear to have been studied in detail, but H(PyrIm$^{\mathrm{Me}}$) was identified as a product formed in the reaction of [Cu(PyrIm$^{\mathrm{Me}}$)$_2$] with 1:1 NH_3/H_2 [113]. In addition, H(amd$^{s\mathrm{Bu}}$) was the only byproduct in Cu_3N ALD using [Cu$_2$(amd$^{s\mathrm{Bu}}$)$_2$] and NH_3, and the use of $^{15}NH_3$ confirmed that the source of nitrogen in Cu_3N was ammonia, rather than the amidinate ligands [119]. Beyond the field of metal ALD, it is relevant to note that ammonolysis (using NH_3 or an ammonium halide) has also been employed for the synthesis of molecular nitrido complexes of a range of mid- and early-transition metals including Os, W, Ta and Ti [126, 127], and typical metal precursors in this reactivity are alkyl [128, 129], alkylidene [130], alkylidyne, amido and chloro complexes [126, 127].

Table 5. Metal precursor / co-reactant combinations that have been used for metal ALD or pulsed-CVD and employ amine or hydrazine co-reactants. This table focuses on initial literature reports for each metal precursor / co-reactant combination. The first column of the table indicates whether ALD or pulsed-CVD is claimed, although in many cases ALD is claimed without demonstration of self-limiting growth.

Deposited Metal (ALD or CVD)	Substrate	Metal Precursor	Co-reactant	Reaction Temp. (°C)	Year	Reference
Co (ALD)	H-term Si or SiO_2	$Co(amd^{iPr})_2$	NH_3	350	2010	Kim *et al.* [28]
Co (ALD)	H-term Si	$(allyl^{tBu})Co(CO)_3$	$N_2H_2Me_2$	140	2012	Kwon *et al.* [20]
Cu (decomp)[a]	glass	$Cu(PyrIm^R)_2$ (R = Me, Et)	1:1 NH_3/H_2	180	2004	Grushin *et al.* [113]
Cu + Cu_3N (nd)[b]	SiO_2 or Al_2O_3	$Cu(hfac)_2$	NH_3 or H_2O then NH_3	283	2006	Törndahl *et al.* [120]
Cu (nd)[c]	Ru	$Cu_2(amd^{sBu})_2$	NH_3	280	2006	Gordon *et al.* [119]
Cu (indirect)[d]	Ru	$Cu_2(amd^{sBu})_2$	NH_3 to Cu_3N film, then H_2	160, then 225	2006	Gordon *et al.* [119]
Cu (ALD)	SiO_2	$Cu(OCHMeCH_2NMe_2)_2$	HCO_2H, then N_2H_4	100-180	2011	Winter *et al.* [131]
Ni (ALD)	Si, SiO_2	$Ni(dmamb)_2$	NH_3	300	2011	Kim *et al.* [29]
Ni (ALD)	SiO_2	$Ni(OCHMeCH_2NMe_2)_2$	HCO_2H, then N_2H_4	180	2011	Winter *et al.* [131]
Ru (CVD/ALD mix)	SiO_2 or WN	$(amd^{tBu})_2Ru(CO)_2$	NH_3	300	2007	Gordon *et al.* [118]

(a) experimental details were not provided. (b) not determined at this temperature, although CuN ALD was demonstrated at 247 °C. (c) not determined. (d) deposition was achieved in two separate steps (see co-reagents and reaction temperatures in the table).

2.5.2. Hydrazines

In contrast to the reactions described above, cobalt metal ALD was achieved at the low temperature of 140 °C using $[(allyl^{tBu})Co(CO)_3]$ in combination with dimethylhydrazine (the authors did not disclose whether 1,1- or 1,2-dimethylhydrazine was used; Table 5) [20]. This low temperature would appear to preclude any mechanistic proposal involving the intermediate formation of a cobalt nitride film, since it would be expected to be stable under the reaction conditions (*vide supra*). However, initial formation of a surface-bound cobalt hydrazide species ($[Co]–C_3H_4{}^tBu + N_2H_2Me_2 \rightarrow [Co]–N_2HMe_2 + H_2C{=}CH\text{-}CH_2{}^tBu$) seems likely [132, 133].

Recently, Winter *et al.* reported copper metal ALD at the uncommonly low temperature of 100 °C using $[Cu(OCHMeCH_2NMe_2)_2]$ in combination with two different co-reactants applied in sequence after the metal precursor pulse; formic acid and hydrazine [131]. Hydrazine on its own proved to be unreactive towards the copper(II) precursor at 100 °C. However, initial ALD growth studies using just $[Cu(OCHMeCH_2NMe_2)_2]$ and formic acid

yielded soluble green films presumed to be copper(II) formate. Copper(II) formate tetrahydrate is stable below 225 °C, but an aqueous solution of copper formate was previously reported to undergo rapid room temperature decomposition to copper metal upon addition of hydrazine [134]. The ability of hydrazine to reduce copper formate to copper metal in solution is clearly mirrored at the surface during ALD. Winter also reported preliminary reactions that broaden the scope of this reactivity. Firstly, copper metal ALD was achieved using [Cu(OCHMeCH$_2$NMe$_2$)$_2$], acetic acid and hydrazine, implying that a range of protic acids could potentially be employed in place of formic acid. Secondly, nickel metal films were deposited using [Ni(OCHMeCH$_2$NMe$_2$)$_2$], formic acid and hydrazine at 175 °C [131].

2.6. $C_xH_yO_z$ co-reactants

2.6.1. Formalin

Formalin [a solution of formaldehyde (HCHO) in water, often containing a stabilizer such as methanol to inhibit polymerization], gyloxylic acid (HC(O)CO$_2$H), formic acid (HCO$_2$H), and alcohols (ROH) have all been used as co-reactants for metal ALD or pulsed-CVD (Table 6). Use of the first two co-reactants likely draws inspiration from their prevalent use as reducing agents in late transition metal electroless deposition (other common reducing agents for this application are NaH$_2$PO$_2$, NaBH$_4$, [NH$_3$OH]Cl, N$_2$H$_4$, and Me$_2$HNBH$_3$) [135-138].

Palladium ALD on an alumina substrate using [Pd(hfac)$_2$] and formalin has been studied in detail using QCM [139] and IR spectroscopic [140, 141] measurements, and on the basis of these studies, the reaction steps in equations 4-8 ([Al] denotes the alumina surface, excluding the terminating bond, [Pd] denotes the palladium surface) have been proposed. At 200 °C, some decomposition of [Al]-hfac groups to yield [Al]-O$_2$CCF$_3$ groups was also observed by IR spectroscopy [141], but this reactivity is not included in the basic series of reactions shown below.

At early stages of deposition (i.e. deposition on alumina) at 200 °C:

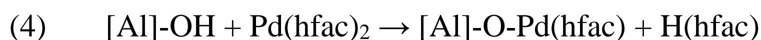

(4) [Al]-OH + Pd(hfac)$_2$ → [Al]-O-Pd(hfac) + H(hfac)

(5) [Al]-OH + H(hfac) → [Al]-hfac + H$_2$O

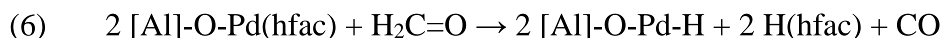

(6) 2 [Al]-O-Pd(hfac) + $H_2C{=}O$ → 2 [Al]-O-Pd-H + 2 H(hfac) + CO

At later stages of deposition (i.e. deposition on palladium) at 100 or 200 °C:

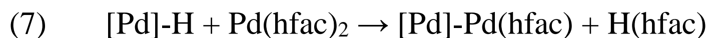

(7) [Pd]-H + $Pd(hfac)_2$ → [Pd]-Pd(hfac) + H(hfac)

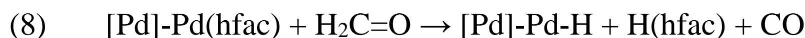

(8) [Pd]-Pd(hfac) + $H_2C{=}O$ → [Pd]-Pd-H + H(hfac) + CO

The role of formaldehyde is suggested simply to be the formation of palladium-bound atomic hydrogen, given that QCM measurements during co-reactant addition were identical for formaldehyde and H_2. The [Al]-hfac species formed in reaction 5 above were identified as the cause of the long nucleation period for palladium ALD on Al_2O_3 using this precursor / co-reactant combination. However, they could be removed by reaction with $AlMe_3$ (converting [Al]-hfac to [Al]-Me) after each formalin pulse, decreasing the number of cycles required for nucleation and reducing the temperature required in early stages of the deposition from 200 °C to 100 °C.

Table 6. Metal precursor / co-reactant combinations that have been used for metal ALD or pulsed-CVD and employ $C_xH_yO_z$ co-reactants. This table focuses on initial literature reports for each metal precursor / co-reactant combination. The first column of the table indicates whether ALD or pulsed-CVD is claimed, although in many cases ALD is claimed without demonstration of self-limiting growth.

Deposited Metal (ALD or CVD)	Substrate	Metal Precursor	Co-reactant	Reaction Temp. (°C)	Year	Reference
Pd (ALD)	Al_2O_3, SiO_2, glass	$Pd(hfac)_2$	Formalin	200 (100 after Pd nucleation)	2006	Elam *et al.* [139]
Pd (ALD)	Al_2O_3, SiO_2, glass	$Pd(hfac)_2$	Formalin, then $AlMe_3$	100	2009	George *et al.* [140]
Pd (CVD)	SAM[a]	$Pd(hfac)_2$	Glyoxylic Acid	210	2003	Senkevich *et al.* [86]
Cu (CVD)	Ru as well as TiN, TaN, TaCN, SiO_2	Cu{RC(O)CHC(NCH$_2$CH$_2$-OSiMe$_2$CH=CH$_2$)R} (R = Me or CF_3)	Formic Acid	125 on Ru; 225-250 on other	2008	Norman *et al.* [142]
Ag nanoparticles (LIALD or LICVD)	Glass, SiN, holey carbon TEM grid	(hfac)Ag(COD) in toluene	PrOH	110-150	2010	Chalker *et al.* [143]

(a) SAM grown on the native oxide of silicon using bis[3-(triethoxysilyl)propyl]tetrasulfide.

2.6.2. *Glyoxylic acid*

Glyoxylic acid was used for palladium metal deposition from $Pd(hfac)_2$ at 200 °C. However, as the authors pointed out, this co-reactant decomposes thermally in the gas phase to CO_2 and formaldehyde above 200 °C [144], so it is fairly likely that glyoxylic acid simply serves as an *in-situ* source of formaldehyde.

2.6.3. Formic acid

Formic acid has been used as a co-reactant for copper pulsed-CVD using $[Cu\{RC(=O)CHC(=NCH_2CH_2\text{-}OSiMe_2CH=CH_2)R\}]$ (R = Me or CF_3; deposition at 125 °C on Ru, 225 °C on TiN, TaN and TaCN, and 250 °C on SiO_2) [142]. This $C_xH_yO_z$ co-reactant has previously been employed for late transition metal (e.g. Pt/Ru alloy) [145] electroless deposition, but is not a common choice. However it does decompose to either (a) H_2 and CO_2 or (b) H_2O and CO in combination with a range of metal surfaces and complexes, and in some cases, only the former reaction is observed (e.g. decomp. of 1:1 HCO_2H/H_2O over 5% Ir/C at 110-200 °C or 1% Au/SiO_2 at 200 °C) [146-150]. On copper surfaces, formic acid decomposition also yields primarily H_2 and CO_2, and this reaction becomes significant in the 150-200 °C range; the reaction involves the steps shown in equations 9-11 ([Cu] denotes the copper surface) [151-154]. Copper pulsed-CVD using $[Cu\{RC(=O)CHC(=NCH_2CH_2\text{-}OSiMe_2CH=CH_2)R\}]$ (R = Me or CF_3) and formic acid likely involves reactions between the precursor and surface-bound atomic hydrogen ([Cu]-H formed during formic acid decomposition) [142]. However, decomposition of an intermediate surface-bound formic acid or formate complex that retains intact or fragmented ligands from the metal precursor cannot be ruled out. Alternative more circuitous mechanisms are also conceivable, given that formic acid is effective for the reduction of Cu_2O to Cu metal at around 150 °C (the reaction byproducts are CO_2 and H_2O) [155-157].

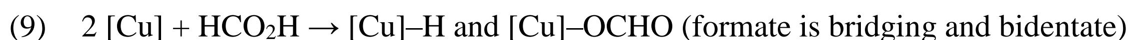

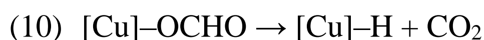

2.6.4. Alcohols

Propanol was recently reported as a co-reactant for silver nanoparticle liquid-injection pulsed-CVD from [(hfac)Ag(COD)] at 110-150 °C [143]. Related silver liquid-injection CVD (not pulsed-CVD) processes were reported using [(hfac)Ag(COD)], [(hfac)Ag(PMe_3)], or $AgNO_3$ dissolved in methanol or ethanol at temperatures in the 150-400 °C range [158-160]. With the hfac precursors but not with $AgNO_3$, the mechanism is considered to involve alcohol dehydrogenation, which is catalyzed by a range of transition metal surfaces and complexes [161]. Consistent with this proposal, Ag LICVD using [(hfac)Ag(COD)] and ethanol ($MeCH_2OH$) yielded free acetaldehyde (MeCHO) at 200 °C and above. However, H_2 was not observed below 350 °C, indicating that at 350 °C and below, both hydrogen atoms provided by ethanol are eliminated as H(hfac). Plausible reaction steps, the first two of which have been proposed to occur during MeOH dehydrogenation to formaldehyde at a silver surface [161], are shown in equations 12-14 ([Ag] denotes the silver surface). Liquid injection CVD using alcoholic precursor solutions has also been reported for metallic Fe, Ru, Co, Ni, Pt and Cu deposition [4].

(12) $2\,[Ag] + RCH_2OH \rightarrow [Ag]\text{-}H + [Ag]\text{-}OCH_2R$

(13) $[Ag]\text{-}OCH_2R \rightarrow [Ag]\text{-}H + RCHO$

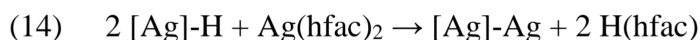
(14) $2\,[Ag]\text{-}H + Ag(hfac)_2 \rightarrow [Ag]\text{-}Ag + 2\,H(hfac)$

2.7. Zinc metal

Copper and molybdenum deposition has been achieved using alternating pulses of a metal chloride (CuCl or $MoCl_5$) and zinc vapours at 400-500 °C (Table 7). High temperatures were required since zinc metal and CuCl are low vapour-pressure solids. The lack of self-limiting behaviour was attributed to dissolution of zinc in copper and molybdenum and etching of molybdenum by reaction (comproportionation) with $MoCl_5$. The reactions proposed to be involved are shown in equations 15-17.

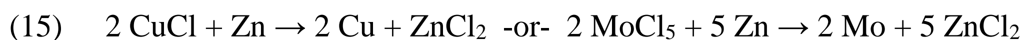
(15) $2\,CuCl + Zn \rightarrow 2\,Cu + ZnCl_2$ -or- $2\,MoCl_5 + 5\,Zn \rightarrow 2\,Mo + 5\,ZnCl_2$

(16) $M + x\,Zn \rightarrow M(Zn)_x$ (M = Cu or Mo and $M(Zn)_x$ is an alloy with zinc)

(17) $x\ \mathrm{Mo} + (5\text{-}x)\ \mathrm{MoCl_5} \rightarrow 5\ \mathrm{MoCl_{(5\text{-}x)}}$

Table 7. Metal precursor / co-reactant combinations that have been used for metal ALD or pulsed-CVD and employ Zn metal, $ZnEt_2$ or $AlMe_3$ as the co-reactant. This table focuses on initial literature reports for each metal precursor / co-reactant combination. The first column of the table indicates whether ALD or pulsed-CVD is claimed, although in many cases ALD is claimed without demonstration of self-limiting growth.

Deposited Metal (ALD or CVD)	**Substrate**	**Metal Precursor**	**Co-reactant**	**Reaction Temp. (°C)**	**Year**	**Reference**
Cu (containing 3% Zn) (ALD)	Al_2O_3	CuCl	Zn	440-500	1997	Ritala *et al.* [162]
Mo (containing < 1% Zn) (CVD)	Al_2O_3 or glass	$MoCl_5$	Zn	400-500	1998	Juppa *et al.* [30]
Cu (ALD)	Oxidized Si	$Cu(OCHMeCH_2NMe_2)_2$	$ZnEt_2$	100-120	2009	Sung and Fischer *et al.* [26]
Cu (containing ~10% Zn) (CVD)	SiO_2, Ru or Ta	$Cu(PyrIm^{Et})$	$ZnEt_2$	130	2010	Emslie and Clendenning *et al.* [163]
Cu (containing a substantial percentage of Al) (CVD)	Ru or Ta	$Cu(PyrIm^{Et})$ or $Cu(IPSA)_2$	$AlMe_3$	120-180	2010	Emslie and Clendenning *et al.* [163, 164]

2.8. Diethylzinc

In 2009, Sung and Fischer *et al.* reported the use of diethylzinc ($ZnEt_2$) for copper metal ALD at 100-120 °C using $[Cu(OCHMeCH_2NMe_2)_2]$ as the metal precursor (Table 7) [26]. Shortly thereafter, we reported similar results using $[Cu(PyrIm^{Et})_2]$ in combination with $ZnEt_2$ at 130 °C (Table 7; lower substrate temperatures were not feasible using $[Cu(PyrIm^{Et})_2]$ due to a minimum delivery temperature of 120 °C). However, in this case, approximately 10% zinc incorporation was observed and self-limiting growth could not be achieved. At a temperature of 130 °C, Cu ALD was proposed to occur concurrently with a parasitic zinc CVD process, and consistent with this hypothesis, zinc CVD from $ZnEt_2$ was observed to become significant on a copper substrate at temperatures above 120 °C. Sung and Fischer *et al.* also reported significant zinc incorporation during attempted copper ALD using using $[Cu(OCHMeCH_2NMe_2)_2]$ and $ZnEt_2$ at 130 °C, and surface-based decomposition of $ZnEt_2$ to yield zinc metal has been suggested to occur during the $ZnEt_2/H_2O$ ALD ZnO process, which operates from 120-180 °C [165].

The mechanism of copper metal ALD or pulsed-CVD using $ZnEt_2$ as the co-reactant has not been investigated directly. However, a detailed study of the reactions between [Cu(PyrIm^{iPr})$_2$] and $ZnEt_2$ in toluene solution has been reported [166]. These reactions were monitored primarily by solution NMR spectroscopy (Figure 2), and the reaction byproducts and intermediates [Cu_2(PyrIm^{iPr})$_2$] PyrIm^{iPr}-Et, [(PyrIm^{iPr})ZnEt] and [Zn(PyrIm^{iPr})$_2$] were synthesized independently to allow conclusive identification as well as assessment of their thermal stability and volatility. Based on these studies, the reaction pathways shown in Scheme 1 were proposed.

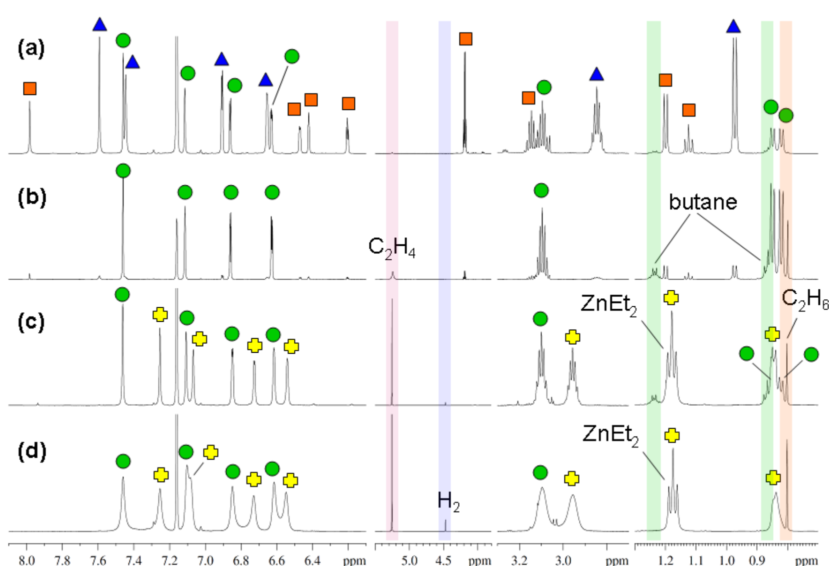

Figure 2. Selected regions of the 600 MHz ^{1}H NMR spectra for reactions between [Cu(PyrIm^{iPr})$_2$] or [Cu_2(PyrIm^{iPr})$_2$] with $ZnEt_2$ at 20 °C in C_6D_6: (a) [Cu(PyrIm^{iPr})$_2$] + 0.3 equiv. $ZnEt_2$ after 15 minutes, (b) [Cu(PyrIm^{iPr})$_2$] + 1 equiv. $ZnEt_2$ after 15 minutes, (c) [Cu(PyrIm^{iPr})$_2$] + 5 equiv. $ZnEt_2$ after 1 hour, (d) [Cu_2(PyrIm^{iPr})$_2$] + 5 equiv. $ZnEt_2$ after 15 minutes. In spectra (c) and (d), the ZnCH_2 peak (0.18 ppm) for ethyl groups exchanging between [(PyrIm^{iPr})ZnEt] and $ZnEt_2$ is not shown (only one ethyl peak is observed because [(PyrIm^{iPr})ZnEt] is in rapid equilibrium with $ZnEt_2$ and [Zn(PyrIm^{iPr})$_2$] in solution at room temperature). Shaded areas highlight chemical shift positions for gaseous byproducts (H_2, ethylene, ethane and *n*-butane). Symbols mark different reaction intermediates and byproducts: triangle = [Cu_2(PyrIm^{iPr})$_2$], square = PyrIm^{iPr}-Et, cross = [(PyrIm^{iPr})ZnEt], circle =

$[Zn(PyrIm^{iPr})_2]$. This figure was reproduced with permission from reference [166]. Copyright 2010 American Chemical Society.

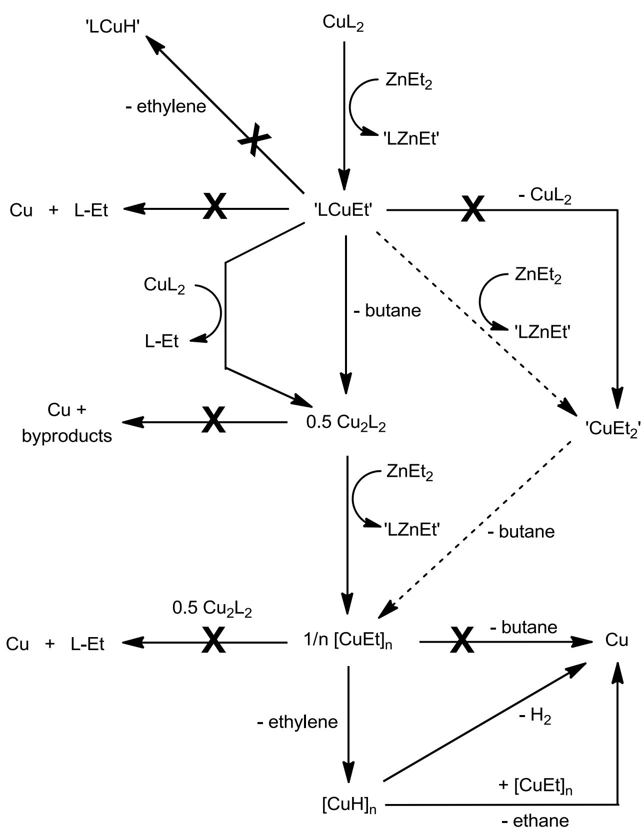

Scheme 1. Reaction pathways for room temperature copper metal deposition from $[Cu(PyrIm^{iPr})_2]$ with $ZnEt_2$ ($L = PyrIm^{iPr}$). Reactions marked with an X do not occur. Dotted arrows represent reactions that cannot be ruled out in the presence of a large excess of $ZnEt_2$. This figure was reproduced with permission from reference [166]. Copyright 2010 American Chemical Society.

The fundamental steps involved in this reactivity are outlined below ($L = PyrIm^{iPr}$). Note that $[ZnL_2]$ is also a potential byproduct in the reactions of $ZnEt_2$ with $[CuL_2]$. This byproduct could form directly *via* reaction of [LZnEt] with $[CuL_2]$ or $[Cu_2L_2]$, although in solution, these reactions were shown to be much slower than the analogous reactions involving $ZnEt_2$.

Alternatively, [ZnL_2] could form from [LZnEt] by ligand redistribution ([LZnEt] → [ZnL_2] + $ZnEt_2$); this reaction was shown to occur upon attempted sublimation of pure solid samples of [LZnEt] at 70 °C under dynamic vacuum (~10 mTorr), to the extent that the sublimed product was pure [ZnL_2].

(1) Ligand transfer between the copper precursor and $ZnEt_2$ (e.g. CuL_2 + $ZnEt_2$ → LCuEt + LZnEt).

(2) Rapid consumption of the in-situ generated copper(II) alkyl complex (LCuEt) by one of three pathways: (2a) reaction with remaining CuL_2 (LCuEt + CuL_2 → Cu_2L_2 + L-Et), (2b) reaction with another molecule of LCuEt (2 LCuEt → Cu_2L_2 + *n*-butane), or (2c) reaction with a second molecule of the $ZnEt_2$ co-reactant (LCuEt + $ZnEt_2$ → $CuEt_2$ + LZnEt). Pathway '2a' is favored when $ZnEt_2$ is added slowly, since CuL_2 is present in large excess relative to LCuEt or $ZnEt_2$. By contrast, pathway '2b' or perhaps pathway '2c' is favored when an excess of $ZnEt_2$ is added rapidly to a solution of CuL_2. Pathways '2a' and '2b' involve bimolecular reductive elimination. Pathway '2c' involves a second ligand transfer between copper and zinc.

(3) Formation of ethyl copper. The product of reactions '2a' and '2b' above is Cu_2L_2, and this compound was shown to react with $ZnEt_2$ to yield 'CuEt' (0.5 Cu_2L_2 + $ZnEt_2$ → 'CuEt' + LZnEt). The product of reaction '2c' above is $CuEt_2$. If this product is formed, in order to be consistent with experimental findings, it must decompose to give 'CuEt' and *n*-butane as the only reaction products (2 $CuEt_2$ → 2 'CuEt' + *n*-butane).

(4) Decomposition of highly thermally unstable ethyl copper to copper metal by a combination of β-hydride elimination ('CuEt' → 'CuH' + ethylene) and reductive elimination [(a) 'CuEt' + 'CuH' → 2 Cu + ethane, and (b) 2 'CuH' → 2 Cu + H_2].

There are likely to be both similarities and differences between the solution reactions described above and the surface reactions occurring during ALD/pulsed-CVD. However since the ALD/pulsed-CVD reactions in question were conducted at low temperature, similarities are more likely than for ALD/pulsed-CVD reactions occurring at high temperature (e.g. > 200 °C). Overall, it seems probable that ligand transfer between copper and zinc plays a key role in both the solution and surface reactivity, and that thermal decomposition reactions of in-situ

generated alkyl copper species are responsible for reduction of copper(II) in the starting complex to copper(0) in the metal film. That said, comproportionation reactions that may occur on a metal surface (e.g. CuL_2 + [Cu] → 2 [Cu]L or Cu_2L_2, or LCuEt + [Cu] → [Cu]L + [Cu]Et) are less likely to be involved in solution reaction studies, unless the observed 'solution' reactivity occurs primarily at the surface of growing metal particles or film.

The thermodynamics of potential reactions involved in copper metal ALD/pulsed-CVD using $ZnEt_2$ in combination with [$Cu(OCHMeCH_2NMe_2)_2$], [$Cu(PyrIm^R)_2$] (R = Et and ^{i}Pr), [$Cu(acac)_2$], [$Cu(hfac)_2$], and $CuCl_2$ were the subject of a recent computational study [167]. Reaction classes considered in this study were ligand exchange, reductive elimination and disproportionation. Additional possibilities such as β-hydride elimination, which is known to play a key role in the decomposition of various copper(I) alkyl complexes [166, 168, 169], and bond homolysis were not included.

In general, the reaction pathways calculated to operate during metal deposition match those observed in solution for [$Cu(PyrIm^{iPr})_2$] and $ZnEt_2$. For example: (a) ligand exchange reactions between CuL_2 and $ZnEt_2$ and/or Cu_2L_2 and $ZnEt_2$ were found to be a prerequisite for reduction to copper metal, (b) both *n*-butane and L-Et reductive elimination were found to be thermodynamically favorable from LCuEt (2 LCuEt → Cu_2L_2 + *n*-butane, or LCuEt + CuL_2 → Cu_2L_2 + L-Et; the former reaction is more thermodynamically favorable), and (c) L-Et reductive elimination from the proposed copper(I) intermediate, Cu_2LEt, was found to be thermodynamically unfavorable (L-Et was not formed in solution reactions of Cu_2L_2 with $ZnEt_2$). Interestingly, Elliott *et al.* also found that of all the metal precursors studied, only [$Cu(PyrIm^R)_2$] precursors are likely to undergo comproportionation upon contact with a copper metal surface (i.e. [Cu] + CuL_2 → [Cu]-L). However, the authors reached the surprising conclusion that $CuEt_2$ is stable towards reduction and will not yield metallic copper, which does not seem to be supported by their own data and is contrary to the available experimental evidence to show that copper(II) alkyl complexes are typically highly thermally unstable. For example, reaction of $CuCl_2$ with RMgBr (R = Me or Et), $MgMe_2$ or MeLi has been reported to yield only the copper(I) alkyl product $[CuR]_n$ and R_2 (ethane or *n*-butane), presumably *via* in-situ generated 'ClCuR' or 'CuR_2' [170, 171]. Similarly, reaction of $LiCu^nBu_2$ with O_2 or nitrobenzene was reported to yield $[Cu^nBu]_n$ with *n*-octane as the primary byproduct [172], and oxidation of [(NHC)CuR] (R = Me or Et) with AgOTf resulted in rapid formation of

[(NHC)Cu(OTf)] and R_2 (ethane or *n*-butane) *via* a pathway that does not appear to involve either alkyl group transfer to silver(I) or alkyl radicals [173].

2.9. Trimethylaluminium

Trimethylaluminium was investigated as a co-reactant for copper metal ALD/pulsed-CVD from [Cu(PyrIm^{Et})$_2$] and [Cu(IPSA)$_2$] at 120-180 °C. In both cases, copper films were deposited, but contained significant percentages of aluminium (Table 7). For example, reaction of [Cu(IPSA)$_2$] with $AlMe_3$ at 150 °C using a ruthenium substrate yielded a film with the following composition by XPS after air exposure: 54% Cu, 16% Al, 27% O, 3% C and <0.5% N. The oxygen content of the film likely arose from aerial oxidation of metallic aluminium, and the low conductivity of the film is consistent with the presence of insulating Al_2O_3. While the goal of this work was pure copper deposition, it is worth noting that B, Al, In, Pd, Au, Ag, Cr, Ti, Nb and Mn have been cited as copper alloying elements of particular interest for interconnect applications, and Zn, V, C, Mg, P and Sn were listed as additional elements worthy of further investigation in this role [174].

Solution reaction studies on the mechanism of copper deposition from [Cu(PyrIm^{Et})$_2$] and $AlMe_3$ yielded a reaction scheme analogous to that obtained using $ZnEt_2$, except that unlike ethyl copper, methyl copper cannot undergo β-hydride elimination, so it decomposed directly by reductive elimination of ethane. Polyalkylaluminium co-reactants do not appear to have been used successfully for pure metal ALD/pulsed-CVD. However, it is notable that they have considerable precedent as reagents for metal nanoparticle formation [175] and zero-valent metal complex formation; for example, [Ni(COD)$_2$] [176], [Pd(C_2H_4)(PPh_3)$_2$] [177], [Fe(COT)$_2$] [178] and [Mo(C_2H_4)(dppe)$_2$] [179] are typically prepared by reaction of [M(acac)$_x$] with $AlEt_3$ or $AlEt_2$(OEt) in the presence of appropriate neutral ligands.

3. Solution screening studies for the rapid identification of promising new reaction chemistries for metal ALD/pulsed-CVD.

As highlighted throughout Section 2, many metal ALD/pulsed CVD precursor / co-reactant combinations and their associated reactivities have close relatives in solution reduction chemistry, particularly in the fields of electroless metal deposition, metal nanoparticle synthesis, and low-valent metal complex synthesis. The fundamental reaction steps involved in these reactivities can be expected to exhibit both similarities and differences relative to those involved in metal ALD/pulsed-CVD, with a greater degree of similarity for ALD/pulsed-CVD reactions occurring at low temperature, given that the vast majority of solution reactions are carried out below 150 °C [180]. It is also worth noting that many of the steps involved in 'solution' deposition reactions have the potential to take place primarily at the surface of a growing metal film or particle. These reaction steps would effectively be heterogeneous surface reactions akin to those involved in ALD/pulsed-CVD, except that they would occur at a solid-liquid interface rather than a solid-gas interface.

The explicit use of solution screening reactions to identify potential new ALD/pulsed-CVD precursor / co-reactant combinations is not commonly described. However, we recently reported screening reactions of this type to evaluate the effectiveness of the potential co-reactants $ZnEt_2$, $AlMe_3$, BEt_3, B_2Pin_2, Sn_2Me_6 and Si_2Me_6 for copper [163, 164] and nickel [164] metal ALD/pulsed-CVD. The copper(II) and nickel(II) precursor complexes used in this work are shown in Figures 3 and 4.

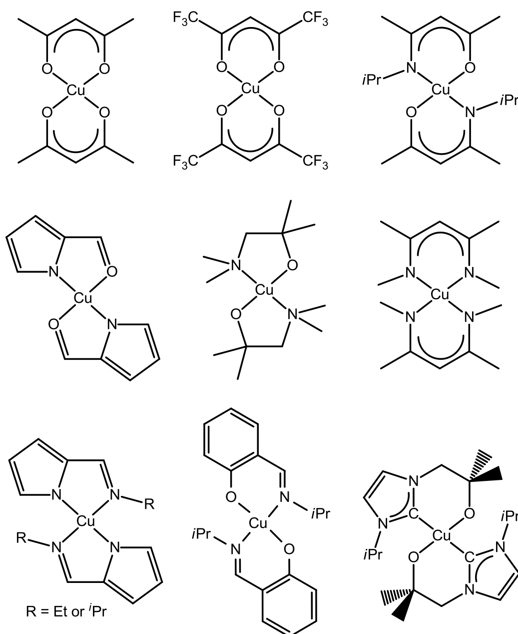

Figure 3. Homoleptic copper(II) complexes used in solution screening reactions with $ZnEt_2$, $AlMe_3$, BEt_3, B_2Pin_2, Sn_2Me_6 and Si_2Me_6 [163, 164].

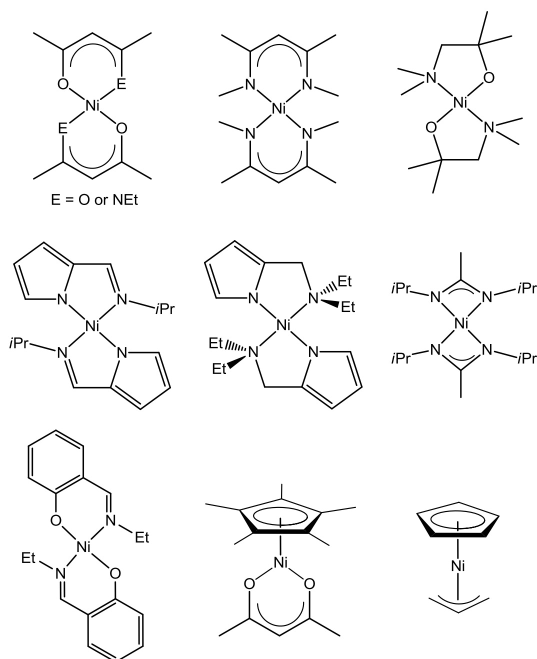

Figure 4. Nickel(II) complexes used in solution screening reactions with $ZnEt_2$, $AlMe_3$, BEt_3, B_2Pin_2, Sn_2Me_6 and Si_2Me_6 [164].

Key findings from these solution studies were: (1) for both copper and nickel, the trend for co-reactant reactivity was $ZnEt_2 > AlMe_3 >> BEt_3 \approx B_2Pin_2 > Sn_2Me_6 > Si_2Me_6$ [163, 164], and (2) in general, the nickel(II) precursors reacted with all co-reactants at higher temperatures than their copper(II) analogues [164]. These trends were reflected in subsequent ALD/pulsed-CVD growth studies: (1) copper (containing $\geq$ 10% Zn or Al) pulsed-CVD was achieved using $ZnEt_2$ and $AlMe_3$, but no deposition was observed using BEt_3 [163, 164], and (2) using $ZnEt_2$ and $AlMe_3$, nickel metal deposition was not observed at temperatures successfully employed for copper pulsed-CVD using closely related precursors [164]. These correlations provide support for the usefulness of solution studies for the identification of promising new ALD/pulsed-CVD reactivity, which is of high value given the very time- and resource-intensive nature of

ALD/pulsed-CVD reaction studies. However, it is important to point out that the morphologies of films deposited from solution and by ALD/pulsed-CVD cannot be expected to correlate with one another. In addition, different criteria determine whether reaction byproducts are removed effectively during solution film deposition and ALD/pulsed-CVD; in the former, the byproducts must be soluble, while in the latter the byproducts must be volatile, in addition to being thermally stable in either case. Solution screening studies should therefore be used primarily as a guide to whether the desired reduction chemistry is chemically accessible at moderate temperatures, and to assess the relative reactivities of potential new precursors and/or co-reactants.

4. Concluding remarks

Given the ability of ALD to deposit highly conformal ultra-thin films of uniform thickness, even on high aspect ratio and high surface area substrates, ALD has the potential to become a primary technique for metal film deposition in the semiconductor industry. Furthermore, use of both a metal precursor *and* a co-reactant in ALD and pulsed-CVD endows these techniques with potential for: (a) metal deposition at lower temperatures than are accessible using single-precursor CVD, and (b) deposition of metals that are inaccessible using single-precursor CVD, although current ALD reaction chemistries have rarely exploited the latter feature. Given that the reactions between metal species and co-reactants are central to inorganic and organometallic chemistry, there are clear opportunities for molecular, solution and surface chemists from these disciplines to make major contributions to the development of new ALD/pulsed-CVD reactivities, ideally concurrent with the design and synthesis of tailored metal precursors. However, a large number of challenges stand between the demonstration of new ALD/pulsed-CVD reaction chemistries (those that operate within the desired temperature regime and yield metal films of the desired purity) and commercial applications, and many of these challenges fall more into the domains of materials science, engineering, and process integration. The development of ALD/pulsed-CVD is therefore a multidisciplinary undertaking, and it is hoped that this review will serve to clarify and categorize the current armoury of ALD/pulsed-CVD reaction chemistries, and to highlight the potential contributions that solution-based studies can make towards development and understanding of the field.

Acknowledgements. D.J.H.E. thanks NSERC of Canada for a Discovery Grant and Intel Corporation for funding through the Semiconductor Research Corporation (SRC). J.S.P. thanks the Government of Ontario for an Ontario Graduate Scholarship (OGS).

References

[1] A.C. Jones, M.L. Hitchman, Chemical Vapour Deposition: Precursors, Processes and Applications, RSC Publishing, Cambridge, 2009.

[2] H. Kim, J. Vac. Sci. Technol., B 21 (2003) 2231-2261.

[3] F. Zaera, J. Phys. Chem. Lett. 3 (2012) 1301-1309.

[4] N. Bahlawane, K. Kohse-Höeinghaus, P.A. Premkumar, D. Lenoble, Chem. Sci. 3 (2012) 929-941.

[5] M. Knez, K. Nielsch, L. Niinistö, Adv. Mater. 19 (2007) 3425-3438.

[6] S.M. George, Chem. Rev. 110 (2010) 111-131.

[7] H. Kim, H.-B.-R. Lee, W.-J. Maeng, Thin Solid Films 517 (2009) 2563-2580.

[8] F. Zaera, J. Mater. Chem. 18 (2008) 3521-3526.

[9] R.L. Puurunen, J. Appl. Phys. 97 (2005) 121301.

[10] M. Leskelä, M. Ritala, Angew. Chem. Int. Ed. 42 (2003) 5548-5554.

[11] H.B. Profijt, S.E. Potts, M.C.M. van de Sanden, W.M.M. Kessels, J. Vac. Sci. Technol., A 29 (2011) 050801.

[12] M. Kariniemi, J. Niinistö, M. Vehkamäki, M. Kemell, M. Ritala, M. Leskelä, M. Putkonen, J. Vac. Sci. Technol., A 30 (2012) 01A115.

[13] M. Kariniemi, J. Niinistö, T. Hatanpää, M. Kemell, T. Sajavaara, M. Ritala, M. Leskelä, Chem. Mater. 23 (2011) 2901-2907.

[14] Values to 2 decimal places are from: J.E. Huheey, E.A. Keiter, R.L. Keiter, Inorganic Chemistry: Principles of Structure and Reactivity, fourth ed.; HarperCollins College Publishers, New York, 1993. Values to 1 decimal place are from: L. Pauling, The Nature of the Chemical Bond, third ed.; Cornell University Press, New York, 1960.

[15] P.R. Gadkari, A.P. Warren, R.M. Todi, R.V. Petrova, K.R. Coffey, J. Vac. Sci. Technol., A 23 (2005) 1152-1161.

[16] C. Boragno, F.B. de Mongeot, R. Felici, I.K. Robinson, Phys. Rev. B 79 (2009) 155443.
[17] J. Kim, T.W. Kim, JOM 61 (2009) 17-22.
[18] P. Mårtensson, J.-O. Carlsson, J. Electrochem. Soc. 145 (1998) 2926-2931.
[19] J.-C. Hierso, R. Feurer, J. Poujardieu, Y. Kihn, P. Kalck, Journal of Molecular Catalysis a-Chemical 135 (1998) 321-325.
[20] J. Kwon, M. Saly, M.D. Halls, R.K. Kanjolia, Y.J. Chabal, Chem. Mater. 24 (2012) 1025-1030.
[21] X.R. Jiang, S.F. Bent, J. Phys. Chem. C 113 (2009) 17613-17625.
[22] E. Färm, M. Kemell, M. Ritala, M. Leskelä, Chem. Vap. Deposition 12 (2006) 415-417.
[23] K.J. Park, G.N. Parsons, Appl. Phys. Lett. 89 (2006) 043111.
[24] K.J. Park, J.M. Doub, T. Gougousi, G.N. Parsons, Appl. Phys. Lett. 86 (2005) 051903.
[25] O. Seitz, M. Dai, F.S. Aguirre-Tostado, R.M. Wallace, Y.J. Chabal, J. Am. Chem. Soc. 131 (2009) 18159-18167.
[26] B.H. Lee, J.K. Hwang, J.W. Nam, S.U. Lee, J.T. Kim, S.-M. Koo, A. Baunemann, R.A. Fischer, M.M. Sung, Angew. Chem. Int. Ed. 48 (2009) 4536-4539.
[27] E. Färm, M. Kemell, M. Ritala, M. Leskelä, J. Phys. Chem. C 112 (2008) 15791-15795.
[28] H.-B.-R. Lee, W.-H. Kim, J.W. Lee, J.-M. Kim, K. Heo, I.C. Hwang, Y. Park, S. Hong, H. Kim, J. Electrochem. Soc. 157 (2010) D10-D15.
[29] W.-H. Kim, H.-B.-R. Lee, K. Heo, Y.K. Lee, T.-M. Chung, C.G. Kim, S. Hong, J. Heo, H. Kim, J. Electrochem. Soc. 158 (2011) D1-D5.
[30] M. Juppo, M. Vehkamäki, M. Ritala, M. Leskelä, J. Vac. Sci. Technol., A 16 (1998) 2845-2850.
[31] S.-H. Kim, N. Kwak, J. Kim, H. Sohn, J. Electrochem. Soc. 153 (2006) G887-G893.
[32] M. Knaut, M. Junige, M. Albert, J.W. Bartha, J. Vac. Sci. Technol., A 30 (2012) 01A151.
[33] S.-H. Choi, T. Cheon, S.-H. Kim, D.-H. Kang, G.-S. Park, S. Kim, J. Electrochem. Soc. 158 (2011) D351-D356.
[34] N. Leick, R.O.F. Verkuijlen, L. Lamagna, E. Langereis, S. Rushworth, F. Roozeboom, M.C.M. van de Sanden, W.M.M. Kessels, J. Vac. Sci. Technol., A 29 (2011) 021016.

[35] J. Hämäläinen, T. Sajavaara, E. Puukilainen, M. Ritala, M. Leskelä, Chem. Mater. 24 (2012) 55-60.

[36] T. Aaltonen, M. Ritala, M. Leskelä, Electrochem. Solid-State Lett. 8 (2005) C99-C101.

[37] H.-B.-R. Lee, H. Kim, Electrochem. Solid-State Lett. 9 (2006) G323-G325.

[38] C.-M. Yang, S.-W. Yun, J.-B. Ha, K.-I. Na, H.-I. Cho, H.-B. Lee, J.-H. Jeong, S.-H. Kong, S.-H. Hahm, J.-H. Lee, Jpn. J. Appl. Phys., Part 1 46 (2007) 1981-1983.

[39] F. Deng, R.A. Johnson, P.M. Asbeck, S.S. Lau, W.B. Dubbelday, T. Hsiao, J. Woo, J. Appl. Phys. 81 (1997) 8047-8051.

[40] C. Henkel, S. Abermann, O. Bethge, E. Bertagnolli, Semicond. Sci. Technol. 24 (2009) 125013.

[41] A. Łaszcz, J. Ratajczak, A. Czerwinski, J. Kątcki, N. Breil, G. Larrieu, E. Dubois, Cent. Eur. J. Phys. 9 (2011) 423-427.

[42] M. Dai, J. Kwon, M.D. Halls, R.G. Gordon, Y.J. Chabal, Langmuir 26 (2010) 3911-3917.

[43] E.D. German, M. Sheintuch, J. Phys. Chem. A 109 (2005) 7957-7966.

[44] X.Y. Deng, B.K. Min, A. Guloy, C.M. Friend, J. Am. Chem. Soc. 127 (2005) 9267-9270.

[45] B. Hammer, J.K. Nørskov, Nature 376 (1995) 238-240.

[46] T. Aaltonen, M. Ritala, V. Sammelselg, M. Leskelä, J. Electrochem. Soc. 151 (2004) G489-G492.

[47] S.T. Christensen, J.W. Elam, Chem. Mater. 22 (2010) 2517-2525.

[48] J. Hämäläinen, M. Kemell, F. Munnik, U. Kreissig, M. Ritala, M. Leskelä, Chem. Mater. 20 (2008) 2903-2907.

[49] A.J.M. Mackus, N. Leick, L. Baker, W.M.M. Kessels, Chem. Mater. 24 (2012) 1752-1761.

[50] N. Leick, S. Agarwal, A.J.M. Mackus, W.M.M. Kessels, Chem. Mater. 24 (2012) 3696-3700.

[51] T. Aaltonen, P. Alén, M. Ritala, M. Leskelä, Chem. Vap. Deposition 9 (2003) 45-49.

[52] Y.-S. Min, E.J. Bae, K.S. Jeong, Y.J. Cho, J.-H. Lee, W.B. Choi, G.-S. Park, Adv. Mater. 15 (2003) 1019-1022.

[53] S.K. Dey, J. Goswami, A. Das, W. Cao, M. Floyd, R. Carpenter, J. Appl. Phys. 94 (2003) 774-777.

[54] S.K. Dey, J. Goswami, D.F. Gu, H. de Waard, S. Marcus, C. Werkhoven, Appl. Phys. Lett. 84 (2004) 1606-1608.

[55] T. Aaltonen, M. Ritala, K. Arstila, J. Keinonen, M. Leskelä, Chem. Vap. Deposition 10 (2004) 215-219.

[56] O.-K. Kwon, J.-H. Kim, H.-S. Park, S.-W. Kang, J. Electrochem. Soc. 151 (2004) G109-G112.

[57] S.K. Kim, S.Y. Lee, S.W. Lee, G.W. Hwang, C.S. Hwang, J.W. Lee, J. Jeong, J. Electrochem. Soc. 154 (2007) D95-D101.

[58] T.-K. Eom, W. Sari, K.-J. Choi, W.-C. Shin, J.H. Kim, D.-J. Lee, K.-B. Kim, H. Sohn, S.-H. Kim, Electrochem. Solid-State Lett. 12 (2009) D85-D88.

[59] K. Kukli, J. Aarik, A. Aidla, T. Uustare, I. Jõgi, J. Lu, M. Tallarida, M. Kemell, A.-A. Kiisler, M. Ritala, M. Leskelä, J. Cryst. Growth 312 (2010) 2025-2032.

[60] K. Kukli, M. Ritala, M. Kemell, M. Leskelä, J. Electrochem. Soc. 157 (2010) D35-D40.

[61] S.K. Park, R. Kanjolia, J. Anthis, R. Odedra, N. Boag, L. Wielunski, Y.J. Chabal, Chem. Mater. 22 (2010) 4867-4878.

[62] K. Kukli, M. Kemell, E. Puukilainen, J. Aarik, A. Aidla, T. Sajavaara, M. Laitinen, M. Tallarida, J. Sundqvist, M. Ritala, M. Leskelä, J. Electrochem. Soc. 158 (2011) D158-D165.

[63] K. Kukli, J. Aarik, A. Aidla, I. Jõgi, T. Arroval, J. Lu, T. Sajavaara, M. Laitinen, A.-A. Kiisler, M. Ritala, M. Leskelä, J. Peck, J. Natwora, J. Geary, R. Spohn, S. Meiere, D.M. Thompson, Thin Solid Films 520 (2012) 2756-2763.

[64] Y.L. Chen, C.C. Hsu, Y.H. Song, Y. Chi, A.J. Carty, S.M. Peng, G.H. Lee, Chem. Vap. Deposition 12 (2006) 442-447.

[65] S.-W. Kim, S.-H. Kwon, D.-K. Kwak, S.-W. Kang, J. Appl. Phys. 103 (2008) 023517.

[66] J. Hämäläinen, T. Hatanpää, E. Puukilainen, L. Costelle, T. Pilvi, M. Ritala, M. Leskelä, J. Mater. Chem. 20 (2010) 7669-7675.

[67] T. Aaltonen, M. Ritala, Y.-L. Tung, Y. Chi, K. Arstila, K. Meinander, M. Leskelä, J. Mater. Res. 19 (2004) 3353-3358.

[68] T. Aaltonen, M. Ritala, T. Sajavaara, J. Keinonen, M. Leskelä, Chem. Mater. 15 (2003) 1924-1928.

[69] J. Hämäläinen, F. Munnik, M. Ritala, M. Leskelä, Chem. Mater. 20 (2008) 6840-6846.

[70] S. Lombardo, J.H. Stathis, B.P. Linder, K.L. Pey, F. Palumbo, C.H. Tung, J. Appl. Phys. 98 (2005) 121301.

[71] Z.Y. Liu, S. Fujieda, H. Ishigaki, M. Wilde, K. Fukutani, ECS Trans. 4 (2011) 55-72.

[72] M.W. Tew, J.T. Miller, J.A. van Bokhoven, J. Phys. Chem. C 113 (2009) 15140-15147.

[73] W. Dong, V. Ledentu, P. Sautet, A. Eichler, J. Hafner, Surf. Sci. 411 (1998) 123-136.

[74] Manganese metal ALD has also recently been claimed in the patent literature using $[LMn(CO)_4]$ [L = allyl ($C_3H_2R_3$), azaallyl (C_2NHR_3) or amidinate/guanidinate (CN_2R_3)] precursors in combination with a reducing gas such as hydrogen. However, it is not clear whether this is an example of thermal ALD (e.g. using H_2) or PEALD (using H•): D. Thompson, J. W. Anthis, US 2012/0231164 A1 (2012).

[75] Ligand hydrogenation would likely involve surface Cu-H species, but it is not clear why the resulting Cu-(N^sBu-CHMe-NH^sBu) linkages would react with H(amd^{sBu}) but not H_2, especially given that related Cu-(amidinate) linkages are readily cleaved by H_2.

[76] Z. Li, A. Rahtu, R.G. Gordon, J. Electrochem. Soc. 153 (2006) C787-C794.

[77] Y. Au, Y.B. Lin, H. Kim, E. Beh, Y.Q. Liu, R.G. Gordon, J. Electrochem. Soc. 157 (2010) D341-D345.

[78] B.S. Lim, A. Rahtu, R.G. Gordon, Nat, Mater. 2 (2003) 749-754.

[79] B.S. Lim, A. Rahtu, J.-S. Park, R.G. Gordon, Inorg. Chem. 42 (2003) 7951-7958.

[80] M. Lashdaf, T. Hatanpää, A.O.I. Krause, J. Lahtinen, M. Lindblad, M. Tiitta, Appl. Catal. A 241 (2003) 51-63.

[81] I.K. Igumenov, P.P. Semyannikov, S.V. Trubin, N.B. Morozova, N.V. Gelfond, A.V. Mischenko, J.A. Norman, Surf. Coat. Technol. 201 (2007) 9003-9008.

[82] P. Serp, R. Feurer, R. Morancho, P. Kalck, J. Catal. 157 (1995) 294-300.

[83] J.-C. Hierso, P. Serp, R. Feurer, P. Kalck, Appl. Organomet. Chem. 12 (1998) 161-172.

[84] C. Dussarrat, J. Gatineau, Proc. Electrochem. Soc. 2005-05 (2005) 354-359.

[85] M. Utriainen, M. Kröger-Laukkanen, L.-S. Johansson, L. Niinistö, Appl. Surf. Sci. 157 (2000) 151-158.

[86] J.J. Senkevich, F. Tang, D. Rogers, J.T. Drotar, C. Jezewski, W.A. Lanford, G.-C. Wang, T.-M. Lu, Chem. Vap. Deposition 9 (2003) 258-264.

[87] G.A. Ten Eyck, S. Pimanpang, H. Bakhru, T.-M. Lu, G.-C. Wang, Chem. Vap. Deposition 12 (2006) 290-294.

[88] J.-C. Hierso, C. Satto, R. Feurer, P. Kalck, Chem. Mater. 8 (1996) 2481-2485.

[89] J.-C. Hierso, R. Feurer, P. Kalck, Chem. Mater. 12 (2000) 390-399.

[90] P. Mårtensson, J.-O. Carlsson, Chem. Vap. Deposition 3 (1997) 45-50.

[91] Z. Li, S.T. Barry, R.G. Gordon, Inorg. Chem. 44 (2005) 1728-1735.

[92] S.-W. Kang, J.-Y. Yun, Y.H. Chang, Chem. Mater. 22 (2010) 1607-1609.

[93] J. Hämäläinen, E. Puukilainen, M. Kemell, L. Costelle, M. Ritala, M. Leskelä, Chem. Mater. 21 (2009) 4868-4872.

[94] J. Hämäläinen, T. Hatanpää, E. Puukilainen, T. Sajavaara, M. Ritala, M. Leskelä, J. Mater. Chem. 21 (2011) 16488-16493.

[95] T. Törndahl, M. Ottosson, J.-O. Carlsson, Thin Solid Films 458 (2004) 129-136.

[96] J. Chae, H.-S. Park, S.-W. Kang, Electrochem. Solid-State Lett. 5 (2002) C64-C66.

[97] Copper metal deposition has also been reported at 260-300 °C by exposure of a TaN surface to $[Cu(hfac)_2(H_2O)_x]$, followed by treatment with water vapour and then ethanol vapour; each of these steps was conducted only once and lasted 3-5 minutes: (a) H.-H. Lee, C. Lee, Y.-L. Kuo, Y.-W. Yen, Thin Solid Films 498 (2006) 43-49. (b) Lee, C.; Lee, H.-H. Electrochem. Solid-State Lett. 8 (2005) G5-G7. (c) Lee, C.; Lee, H.-H.; Yen, Y.-W.; Kuo, Y.-L. Electrochem. Solid-State Lett. 8 (2005) G307-G310.

[98] A.J. Hoskin, D.W. Stephan, Coord. Chem. Rev. 233-234 (2002) 107-129.

[99] J.Y. Corey, J. Braddock-Wilking, Chem. Rev. 99 (1999) 175-292.

[100] P.L. Holland, R.A. Andersen, R.G. Bergman, J.K. Huang, S.P. Nolan, J. Am. Chem. Soc. 119 (1997) 12800-12814.

[101] X.Z. Liu, Z.Z. Wu, H. Cai, Y.H. Yang, T.N. Chen, C.E. Vallet, R.A. Zuhr, D.B. Beach, Z.-H. Peng, Y.-D. Wu, T.E. Concolino, A.L. Rheingold, Z.L. Xue, J. Am. Chem. Soc. 123 (2001) 8011-8021.

[102] A. Ludviksson, M. Nooney, R. Bruno, A. Bailey, T.T. Kodas, M.J. Hampden-Smith, Chem. Vap. Deposition 4 (1998) 129-132.

[103] R.K. Grubbs, N.J. Steinmetz, S.M. George, J. Vac. Sci. Technol., B 22 (2004) 1811-1821.

[104] F.H. Fabreguette, Z.A. Sechrist, J.W. Elam, S.M. George, Thin Solid Films 488 (2005) 103-110.

[105] D. Seghete, Jr., G.B. Rayner, A.S. Cavanagh, V.R. Anderson, S.M. George, Chem. Mater. 23 (2011) 1668-1678.

[106] A.M. Lemonds, T. Bolom, W.J. Ahearn, D.C. Gay, J.M. White, J.G. Ekerdt, Thin Solid Films 488 (2005) 9-14.

[107] A.M. Lemonds, J.M. White, J.G. Ekerdt, Surf. Sci. 538 (2003) 191-203.

[108] J.S. Thompson, L. Zhang, J.P. Wyre, D. Brill, Z.G. Li, Organometallics 31 (2012) 7884-7892.

[109] J.S. Thompson, US 7,604,840 B2 (2009).

[110] J.S. Thompson, US 7,632,351 B2 (2009).

[111] J.S. Thompson, C.E. Radzewich, US 7,736,697 B2 (2010).

[112] J.S. Thompson, US 7,776,394 B2 (2010).

[113] V.V. Grushin, W.J. Marshall, Adv. Synth. Catal. 346 (2004) 1457-1460.

[114] K.-H. Park, W.J. Marshall, J. Am. Chem. Soc. 127 (2005) 9330-9331.

[115] K.-H. Park, A.Z. Bradley, J.S. Thompson, W.J. Marshall, Inorg. Chem. 45 (2006) 8480-8482.

[116] J.W. Klaus, S.J. Ferro, S.M. George, Thin Solid Films 360 (2000) 145-153.

[117] (a) S.-H. Kim, E.-S. Hwang, B.-M. Kim, J.-W. Lee, H.-J. Sun, T. E. Hong, J.-K. Kim, H. Sohn, J. Kim, T.-S. Yoon, Electrochem. Solid-State Lett. 8 (2005) C155-C159. (b) ref. 30 and references therein.

[118] H. Li, D.B. Farmer, R.G. Gordon, Y. Lin, J. Vlassak, J. Electrochem. Soc. 154 (2007) D642-D647.

[119] Z. Li, R.G. Gordon, Chem. Vap. Deposition 12 (2006) 435-441.

[120] T. Törndahl, M. Ottosson, J.-O. Carlsson, J. Electrochem. Soc. 153 (2006) C146-C151.

[121] K. Suzuki, T. Kaneko, H. Yoshida, H. Morita, H. Fujimori, J. Alloy. Compd. 224 (1995) 232-236.

[122] A. Leineweber, H. Jacobs, S. Hull, Inorg. Chem. 40 (2001) 5818-5822.

[123] Z.Q. Liu, W.J. Wang, T.M. Wang, S. Chao, S.K. Zheng, Thin Solid Films 325 (1998) 55-59.

[124] M.G. Moreno-Armenta, J. Diaz, A. Martinez-Ruiz, G. Soto, J. Phys. Chem. Solids 68 (2007) 1989-1994.

[125] C.-Y. Wu, W.-H. Lee, S.-C. Chang, Y.-L. Cheng, Y.-L. Wang, J. Electrochem. Soc. 158 (2011) H338-H342.

[126] S. Aguado-Ullate, J.J. Carbó, O. González-del Moral, A. Martín, M. Mena, J.M. Poblet, C. Santamaría, Inorg. Chem. 50 (2011) 6269-6279 and references therein.

[127] K. Dehnicke, J. Strähle, Angew. Chem. Int. Ed. Engl. 31 (1992) 955-978.

[128] M.M.B. Holl, P.T. Wolczanski, J. Am. Chem. Soc. 114 (1992) 3854-3858.

[129] M.M.B. Holl, M. Kersting, B.D. Pendley, P.T. Wolczanski, Inorg. Chem. 29 (1990) 1518-1526.

[130] M.M.B. Holl, P.T. Wolczanski, G.D. Van Duyne, J. Am. Chem. Soc. 112 (1990) 7989-7994.

[131] T.J. Knisley, T.C. Ariyasena, T. Sajavaara, M.J. Saly, C.H. Winter, Chem. Mater. 23 (2011) 4417-4419.

[132] For a 1,2-dimethylhydrazide complex, β-hydride elimination akin to that observed for certain amidinate and guanidinate complexes could provide a pathway to an unstable metal hydride. See for example: (a) T.J.J. Whitehorne, J.P. Coyle, A. Mahmood, W.H. Monillas, G.P.A. Yap, S.T. Barry, *Eur. J. Inorg. Chem.* (2011) 3240-3247. (b) J.P. Coyle, P.A. Johnson, G.A. DiLabio, S.T. Barry, J. Muller, Inorg. Chem. 49 (2010) 2844-2850.

[133] A unique set of hydrazide ligand decomposition pathways have been reported in the chemistry of iridium: Z. Huang, J.R. Zhou, J.F. Hartwig, J. Am. Chem. Soc. 132 (2010) 11458-11460.

[134] P. Ravindranathan, K.C. Patil, Thermochimica Acta 71 (1983) 53-57.

[135] M. Paunovic, Electroless Deposition of Copper, in: M. Schlesinger, M. Paunovic (Eds.) Modern Electroplating, John Wiley & Sons, Hoboken, NJ, USA, 2010, pp. 433-446.

[136] M. Schlesinger, Electroless Deposition of Nickel, in: M. Schlesinger, M. Paunovic (Eds.) Modern Electroplating, John Wiley & Sons, Hoboken, NJ, USA, 2010, pp. 447-458.

[137] I. Ohno, Electroless Deposition of Palladium and Platinum, in: M. Schlesinger, M. Paunovic (Eds.) Modern Electroplating, John Wiley & Sons, Hoboken, NJ, USA, 2010, pp. 477-482.

[138] Y. Okinaka, M. Kato, Electroless Deposition of Gold, in: M. Schlesinger, M. Paunovic (Eds.) Modern Electroplating, John Wiley & Sons, Hoboken, NJ, USA, 2010, pp. 483-498.

[139] J.W. Elam, A. Zinovev, C.Y. Han, H.H. Wang, U. Welp, J.N. Hryn, M.J. Pellin, Thin Solid Films 515 (2006) 1664-1673.

[140] D.N. Goldstein, S.M. George, Appl. Phys. Lett. 95 (2009) 143106.

[141] D.N. Goldstein, S.M. George, Thin Solid Films 519 (2011) 5339-5347.

[142] J.A.T. Norman, M. Perez, S.E. Schulz, T. Waechtler, Microelectron. Eng. 85 (2008) 2159-2163.

[143] P.R. Chalker, S. Romani, P.A. Marshall, M.J. Rosseinsky, S. Rushworth, P.A. Williams, Nanotechnology 21 (2010) 405602.

[144] R.A. Back, S. Yamamoto, Can. J. Chem. 63 (1985) 542-548.

[145] W.E. Mustain, H. Kim, V. Narayanan, T. Osborn, P.A. Kohl, J. Fuel Cell Sci. Tech. 7 (2010) 041013.

[146] K. Tedsree, T. Li, S. Jones, C.W.A. Chan, K.M.K. Yu, P.A.J. Bagot, E.A. Marquis, G.D.W. Smith, S.C.E. Tsang, Nat. Nanotechnol. 6 (2011) 302-307.

[147] D.A. Bulushev, S. Beloshapkin, J.R.H. Ross, Catal. Today 154 (2010) 7-12.

[148] B. Loges, A. Boddien, F. Gärtner, H. Junge, M. Beller, Top. Catal. 53 (2010) 902-914.

[149] M. Grasemann, G. Laurenczy, Energy Environ. Sci. 5 (2012) 8171-8181.

[150] G.V. Smith, F. Notheisz, Heterogeneous Catalysis in Organic Chemistry, Academic Press, San Diego, 1999.

[151] A. Ludviksson, R. Zhang, C.T. Campbell, K. Griffiths, Surf. Sci. 313 (1994) 64-82 and references therein.

[152] On atom thin copper islands on ZnO, surface formate decomposed not only to give CO_2 and H_2, but also to produce CO (presmuably via [Cu]-OCHO --> [Cu]-OH + CO). See: E. Iglesia, M. Boudart, J. Catal. 81 (1983) 214-223.

[153] H. Nakano, I. Nakamura, T. Fujitani, J. Nakamura, J. Phys. Chem. B 105 (2001) 1355-1365.

[154] X.-K. Gu, W.-X. Li, J. Phys. Chem. C 114 (2010) 21539-21547.

[155] I. Kim, J. Kim, J. Appl. Phys. 108 (2010) 102807.

[156] H. Kim, Y. Kojima, H. Sato, N. Yoshii, S. Hosaka, Y. Shimogaki, Mater. Res. Soc. Symp. Proc. 914 (2006) 167-172.

[157] S. Poulston, E. Rowbotham, P. Stone, P. Parlett, M. Bowker, Catal. Lett. 52 (1998) 63-67.

[158] N. Bahlawane, P.A. Premkumar, K. Onwuka, K. Rott, G. Reiss, K. Kohse-Höinghaus, Surf. Coat. Technol. 201 (2007) 8914-8918.

[159] N. Bahlawane, P.A. Premkumar, A. Brechling, G. Reiss, K. Kohse-Höinghaus, Chem. Vap. Deposition 13 (2007) 401-407.

[160] N. Bahlawane, K. Kohse-Höinghaus, T. Weimann, P. Hinze, S. Röhe, M. Bäumer, Angew. Chem. Int. Ed. 50 (2011) 9957-9960.

[161] T. Watanabe, M. Ehara, K. Kuramoto, H. Nakatsuji, Surf. Sci. 603 (2009) 641-646.

[162] M. Juppo, M. Ritala, M. Leskelä, J. Vac. Sci. Technol. A 15 (1997) 2330-2333.

[163] B. Vidjayacoumar, D.J.H. Emslie, S.B. Clendenning, J.M. Blackwell, J.F. Britten, A. Rheingold, Chem. Mater. 22 (2010) 4844–4853.

[164] B. Vidjayacoumar, V. Ramalingam, D.J.H. Emslie, J.M. Blackwell, S.B. Clendenning, ECS Trans. 50 (2012) 53-66.

[165] For discussion, see the introduction of: P.C. Rowlette, C.G. Allen, O.B. Bromley, A.E. Dubetz, C.A. Wolden, Chem. Vap. Deposition 15 (2009) 15-20.

[166] B. Vidjayacoumar, D.J.H. Emslie, J.M. Blackwell, S.B. Clendenning, J.F. Britten, Chem. Mater. 22 (2010) 4854–4866.

[167] G. Dey, S.D. Elliott, J. Phys. Chem. A 116 (2012) 8893-8901.

[168] N.J. Rijs, R.A.J. O'Hair, Organometallics 29 (2010) 2282-2291.

[169] X. Li, A.J. Gellman, D.S. Sholl, J. Chem. Phys. 127 (2007) 144710.

[170] H. Gilman, R.G. Jones, L.A. Woods, J. Org. Chem. 17 (1952) 1630-1634.

[171] K. Wada, M. Tamura, J. Kochi, J. Am. Chem. Soc. 92 (1970) 6656-6658.

[172] G.M. Whitesides, J. SanFilippo, Jr., C.P. Casey, E.J. Panek, J. Am. Chem. Soc. 89 (1967) 5302-5303.

[173] L.A. Goj, E.D. Blue, S.A. Delp, T.B. Gunnoe, T.R. Cundari, J.L. Petersen, Organometallics 25 (2006) 4097-4104.

[174] K. Barmak, C. Cabral, Jr., K.P. Rodbell, J.M.E. Harper, J. Vac. Sci. Technol., B 24 (2006) 2485-2498.

[175] H. Bonnemann, K.S. Nagabhushana, R.M. Richards, in: D. Astruc (Ed.) Nanoparticles and Catalysis, Wiley-VCH, Weinheim, 2008.

[176] R.A. Schunn, S.D. Ittel, M.A. Cushing, Inorg. Synth. 28 (1990) 94-98.

[177] A. Visser, R. van der Linde, R.O. de Jongh, Inorg. Synth. 16 (1976) 127-130.

[178] D.H. Gerlach, R.A. Schunn, Inorg. Synth. 15 (1974) 2-4.

[179] M. Hidai, K. Tominari, Y. Uchida, A. Misono, Inorg. Synth. 15 (1974) 25-28.

[180] In some cases, mechanistic parallels between solution deposition reactions and thermal CVD reactions have been suggested on the basis of shared volatile byproducts, deuterium labeling studies, and/or kinetic isotope effects. See for example: (a) J. Cheon, D.M. Rogers, G.S. Girolami, J. Am. Chem. Soc. 119 (1997) 6804-6813. (b) W.R. Entley, C.R. Treadway, S.R. Wilson, G.S. Girolami, J. Am. Chem. Soc. 119 (1997) 6251-6258. (c) C.D. Tagge, R.D. Simpson, R.G. Bergman, M.J. Hostetler, G.S. Girolami, R.G. Nuzzo, J. Am. Chem. Soc. 118 (1996) 2634-6243. (d) Y.P. Zhang, Z. Yuan, R.J. Puddephatt, Chem.Mater. 10 (1998) 2293-2300.